Electronic Influence of the Thienyl Sulfur Atom on the Oligomerization of Ethylene by Cobalt(II) 6-(Thienyl)-2-(imino)pyridine Catalysis

Claudio Bianchini,*,† Dante Gatteschi,‡ Giuliano Giambastiani,*,† Itzel Guerrero Rios,† Andrea Ienco,† Franco Laschi,§ Carlo Mealli,† Andrea Meli,† Lorenzo Sorace,‡ Alessandro Toti,† and Francesco Vizza†

Istituto di Chimica dei Composti Organometallici (ICCOM-CNR), Via Madonna del Piano 10, 50019 Sesto Fiorentino (Firenze), Italy, Dipartimento di Chimica, Università di Siena, Via Aldo Moro, 53100 Siena, Italy, and Dipartimento di Chimica and UdR INSTM, Università di Firenze, Via della Lastruccia 3, 50019 Sesto Fiorentino (Firenze), Italy

Received October 21, 2006

The position of the sulfur atom in the thienyl group of 6-(thienyl)-2-(imino)pyridine ligands strongly affects the catalytic activity of the corresponding tetrahedral high-spin dihalide Co^{II} complexes in the oligomerization of ethylene to α-olefins upon activation with methylaluminoxane (MAO). Complexes with the sulfur atom in the 3-position of the thienyl ring catalyze the selective conversion of ethylene to 1-butene, while catalysts containing thien-2-yl groups give C_4-C_{14} α-olefins. In situ EPR experiments showed the occurrence of a spin state changeover with the formation of low-spin Co^{II} species upon activation of the catalyst precursors by MAO. DFT calculations suggest that only thien-2-yl rings allow for the coordination of the sulfur atom to the cobalt center in the MAO-activated systems.

Introduction

We have recently communicated that tetrahedral dichloride Co^{II} complexes with (imino)pyridine ligands bearing thiophen-2-yl or benzo[*b*]thiophen-2-yl groups in the 6-position of the pyridine ring (N_2^{2Th}, N_2^{2ThE}, and N_2^{2BT} in Scheme 1) are effective catalyst precursors for the Schulz−Flory oligomerization of ethylene.[1−3] On activation by methylaluminoxane (MAO), these Co^{II} complexes promote the conversion of ethylene into short-chain α-olefins with turnover frequencies (TOFs) as high as 1.4×10^5 mol of C_2H_4 converted (mol of Co)$^{-1}$ h^{-1} bar^{-1}. Under conditions analogous to those of the N_2^{2Th}, N_2^{2ThE}, and N_2^{2BT} catalysts, Co^{II} precursors bearing groups of comparable steric size in the pyridine 6-position, yet with no pendant thienyl group (furanyl, phenyl, or naphthyl) are 5 times less active and are also selective for ethylene dimerization (Scheme 1).[1−3]

Since the sulfur atom in the dichloride Co^{II} precursors does not show any bonding interaction with the metal center in both the solid state and solution,[1] we postulated that the sulfur atom might play a relevant role in the catalytic process only after the tetrahedral precursors are activated by MAO. However, no evidence whatsoever was obtained for S-coordination, and we could also not rule out the occurrence of subtle steric effects, in view of the utmost importance of the latter in insertion polymerization catalysis.[4] Understanding the role of the thienyl group in the oligomerization of ethylene by the present Co^{II} catalysts would be a more important achievement than addressing a chemical curiosity (to date, no other tetrahedral Co^{II} precursor is known to effectively oligomerize ethylene).[5] Indeed, there are other examples in polymerization catalysis where a hemilabile ligand, uncoordinated in the precursor, proves to be of crucial importance for promoting the catalytic reaction as well as driving the selectivity toward a specific product.[6−9] Hessen and co-workers have reported that a mono(cyclopentadienylarene)titanium system can be transformed from a poor ethylene polymerization catalyst into an efficient and selective ethylene trimerization catalyst by attachment of a pendant arene group.[7] Theoretical studies have confirmed that the η^6 coordination of the arene to titanium drives out the initially formed alkene products and stabilizes intermediates for the cyclotrimerization of ethylene to 1-hexene.[8] Even more pertinent to the present piece of chemistry is a work reported by Huang and co-workers, who showed that the introduction of a thien-2-yl group on the cyclopentadienyl ring of a half-sandwich titanium complex generates an efficient and selective catalyst for ethylene trim-

* To whom correspondence should be addressed. E-mail: claudio.bianchini@iccom.cnr.it.

† ICCOM-CNR.

‡ Università di Firenze and UdR INSTM-Firenze.

§ Università di Siena.

(1) Bianchini, C.; Mantovani, G.; Meli, A.; Migliacci, F.; Laschi, F. *Organometallics* **2003**, *22*, 2545.

(2) Bianchini, C.; Giambastiani, G.; Mantovani, G.; Meli, A.; Mimeau, D. *J. Organomet. Chem.* **2004**, *689*, 1356.

(3) Mantovani, G. Doctoral Dissertation, Scuola Normale Superiore di Pisa, 2002.

(4) (a) Ittel, S. D.; Johnson, L. K.; Brookhart, M. *Chem. Rev.* **2000**, *100*, 1169. (b) Gibson, V. C.; Spitzmesser, S. K. *Chem. Rev.* **2003**, *103*, 283. (c) Rappé, A. K.; Skiff, W. M.; Casewit, C. S. *Chem. Rev.* **2000**, *100*, 1435.

(5) (a) Dawson, D. M.; Walker, D. A.; Thornton-Pett, M.; Bochmann, M. *Dalton Trans.* **2000**, 459. (b) Wang, M.; Yu, X.; Shi, Z.; Qian, M.; Jin, K.; Chen, J.; He, R. *J. Organomet. Chem.* **2002**, *645*, 127.

(6) (a) Slone, C. S.; Weinberger, D. A.; Mirkin, C. A. In *Progress in Inorganic Chemistry*; Karlin, K. D., Ed.; Wiley: New York, 1999; p 233. (b) Nandi, M.; Jin, J.; RajanBabu, T. V. *J. Am. Chem. Soc*. **1999**, *121*, 9899. (c) Drent, E.; van Dijk, R.; van Ginkel, R.; van Oort, B.; Pugh, R. I. *Chem. Commun*. **2002**, 964.

(7) (a) Hessen, B. *J. Mol. Catal. A: Chem.* **2004**, *213*, 129. (b) Deckers, P. J. W.; Hessen, B.; Teuben, J. H. *Organometallics* **2002**, *21*, 5122. (c) Deckers, P. J. W.; Hessen, B.; Teuben, J. H. *Angew. Chem., Int. Ed.* **2001**, *40*, 2516.

(8) (a) Blok, A. N. J.; Budzelaar, P. H. M.; Gal, A. W. *Organometallics* **2003**, *22*, 2564. (b) Tobisch, S.; Ziegler, T. *Organometallics* **2005**, *24*, 256.

(9) Huang, J.; Wu, T.; Qian, Y. *Chem. Commun*. **2003**, 2816.

10.1021/om0609665 CCC: $37.00
Publication on Web 01/03/2007

Scheme 1

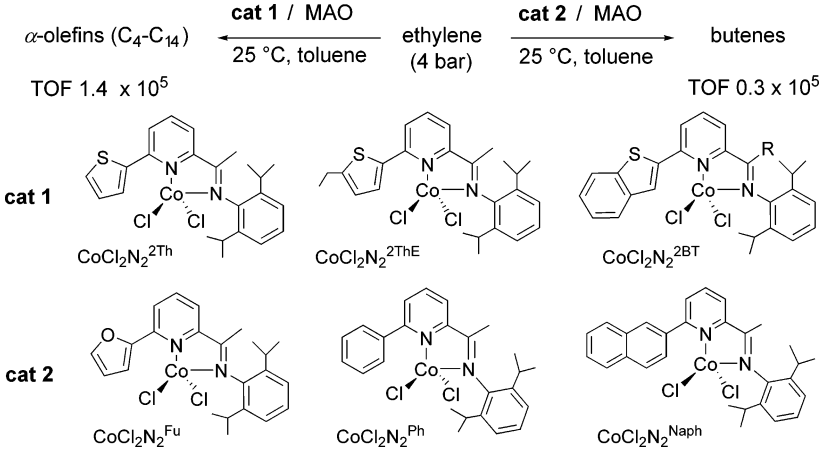

Scheme 2

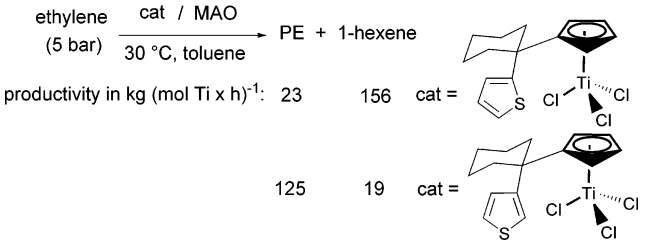

erization to 1-hexene.[9] Notably, shifting the thienyl sulfur atom from the 2-position to the 3-position changed the catalyst selectivity from 1-hexene to polyethylene (PE) (Scheme 2).

A further reason to prove the existence of a "regiochemical thienyl" effect on the polymerization activity of the present Co^{II} catalysts is their industrial relevance in ethylene oligomerization to α-olefins[10] as well as in tandem catalysis for the production of low-density polyethylene.[11] Indeed, establishing a clear-cut relationship between catalytic activity and presence/regiochemistry of hemilabile thienyl groups would provide valuable information for designing improved oligomerization/polymerization catalysts.

In this paper, we report the results of an experimental and theoretical study of ethylene oligomerization by cobalt(II) 6-(organyl)-2-(imino)pyridine dichlorides/MAO, with particular regard to the preliminary activation by MAO. Both known and new complexes have been investigated. Some new complexes contain (imino)pyridine ligands bearing thiophen-3-yl and benzo[*b*]thiophen-3-yl groups, which has allowed us to evaluate the effect of the position of the sulfur atom in the thienyl group on both productivity and selectivity. Other new complexes do not have an organyl group at the pyridine 6-position or have a group capable of forming a robust bond to the cobalt center. We are confident to have obtained convincing evidence of the decisive role exerted by the 6-organyl group and, in particular, by the position of the sulfur atom in the thienyl ring in steering the ethylene oligomerization activity of (imino)pyridine Co^{II} catalysts.

Experimental Section

General Considerations. All air- and/or water-sensitive reactions were performed under nitrogen in flame-dried flasks using standard Schlenk-type techniques. Anhydrous toluene, THF, and Et_2O were obtained by distillation under nitrogen from sodium−benzophenone ketyl. Solid MAO for polymerization was prepared by removing toluene and $AlMe_3$ under vacuum from a commercially available MAO solution (10 wt % in toluene, Crompton Corp.). The MAO solution was filtered on a D4 funnel and evaporated to dryness at 50 °C under vacuum. The resulting white residue was heated further to 50 °C under vacuum overnight. A stock solution of MAO was prepared by dissolving solid MAO in toluene (100 mg mL^{-1}). The solution was used within 3 weeks to avoid self-condensation effects of the MAO. Literature methods were used to synthesize the tetrahedral cobalt complexes $CoCl_2N_2^{2Th}$, $CoCl_2N_2^{2BT}$, $CoCl_2N_2^{2ThE}$, and $CoCl_2N_2^{Ph}$ (N_2^{org} = 6-(organyl)-2-(imino)pyridine).[1,2] All the other reagents and solvents were used as purchased from commercial suppliers. Catalytic reactions were performed with a 500 mL stainless steel reactor, constructed at the ICCOM-CNR (Firenze, Italy), equipped with a magnetic drive stirrer and a Parr 4842 temperature and pressure controller. The reactor was connected to an ethylene reservoir to maintain a constant pressure throughout the catalytic runs. Deuterated solvents for NMR measurements were dried over molecular sieves. ^1H and $^{13}C\{^1H\}$ NMR spectra were obtained on Bruker ACP 200 (200.13 and 50.32 MHz, respectively) and Bruker Avance DRX-400 spectrometers (400.13 and 100.62 MHz, respectively). Chemical shifts are reported in ppm (*δ*) relative to TMS, referenced to the chemical shifts of residual solvent resonances (^1H and ^{13}C). The multiplicities of the $^{13}C\{^1H\}$ NMR spectra were determined with the DEPT 135 technique and quoted as CH_3, CH_2, CH, and C for primary, secondary, tertiary, and quaternary carbon atoms, respectively. X-band EPR spectra were recorded on a Bruker Elexsys E500 spectrometer equipped with a ^4He continuous flow cryostat for operation at variable temperature (4−300 K). Electronic spectra in both the solid state (powdered samples; range 250−1800 nm) and CH_2Cl_2 solution (range 350−1600 nm) were recorded on a Perkin-Elmer Lamda 9 spectrophotometer. Infrared spectra were recorded on a Perkin-Elmer Spectrum BX FT-IR spectrophotometer using samples mulled in Nujol between KBr plates. Molar susceptibilities were measured on solid samples using a Sherwood Scientific MSB AUTO balance. Elemental analyses were performed using a Carlo Erba Model 1106 elemental analyzer with an accepted tolerance of ±0.4 unit on carbon (C), hydrogen (H), and nitrogen (N). Melting points were recorded on a Stuart Scientific SMP3 apparatus. GC analyses of the reaction products were performed on a Shimadzu GC-17 gas chromatograph equipped with a flame ionization detector and a Supelco SPB-1 fused silica capillary column (30 m length, 0.25 mm i.d., 0.25 μm film thickness) for the C6−C20 fraction or a HP-PLOT Al_2O_3 KCl column (50 m length, 0.53 mm i.d., 15 μm film thickness) for the C4−C6 fraction. The GC/MS analyses were

(10) Bianchini, C.; Sommazzi, A.; Mantovani, B.; Santi, R.; Masi, F. (Polimeri Europa) WO 02/34701, 2002.

(11) Bianchini, C.; Frediani, M.; Giambastiani, G.; Kaminsky, W.; Meli, A.; Passaglia, E. *Macromol. Rapid. Commun.* **2005**, *26*, 1218.

performed on a Shimadzu QP2010S apparatus equipped with a column identical with that used for GC analysis.

Synthesis of 1-(6-Bromopyridin-2-yl)ethanone. To a stirred solution of 2,6-dibromopyridine (7.11 g, 30.0 mmol) in Et_2O (130 mL) at −78 °C was added 18.8 mL (30.0 mmol) of a 1.7 M solution of *t*-BuLi in pentane within 10 min. After 30 min of stirring at −78 °C, *N*,*N*-dimethylacetamide (3.1 mL, 33.0 mmol) was added and stirring maintained for 1.5 h. The resulting mixture was warmed to room temperature and treated with water (30 mL). The formed layers were separated, and the organic phase was washed with water (2 × 30 mL). The aqueous layer was extracted with Et_2O (3 × 30 mL). The combined organic layers were dried over Na_2SO_4. Removal of the solvent under reduced pressure gave a yellow oil that was dissolved in petroleum ether and cooled to −20 °C. After 6 h, small yellow pale crystals were separated by filtration (yield 72%). Mp: 44 °C. IR (KBr): ν 1695 cm^{-1} (C═O). ^1H NMR ($CDCl_3$): δ 2.70 (s, 3 H, C(O)CH_3), 7.68 (m, 2 H, CH), 7.98 (dd, J = 6.5, 2.1 Hz, 1 H, CH). $^{13}C\{^1H\}$ NMR ($CDCl_3$): δ 26.4 (1 C, C(O)*C*H_3), 121.1 (1 C, CH), 132.4 (1 C, CH), 139.8 (1 C, CH), 142.0 (1 C, C), 154.9 (1 C, C), 198.5 (1 C, *C*(O)CH_3). Anal. Calcd for C_7H_6BrNO (200.03): C, 42.03; H, 3.02; N, 7.00. Found: C, 42.09; H, 2.90; N, 7.02.

Synthesis of [1-(6-Bromopyridin-2-yl)ethylidene](2,6-diisopropylphenyl)amine (N_2^{Br}). A solution of 1-(6-bromopyridin-2-yl)ethanone (2.40 g, 12.0 mmol), 2,6-diisopropylaniline (tech. 90%; 3.54 g, 18.0 mmol), and formic acid (2 drops) in MeOH (20 mL) was refluxed in an Erlenmeyer flask. After 18 h, the orange solution was cooled to room temperature and allowed to stand for 24 h. During this time, yellow crystals precipitated, which were separated by filtration and washed with MeOH (yield 84%). Mp: 126−128 °C. IR (KBr): ν 1639 cm^{-1} (C═N). ^1H NMR ($CDCl_3$): δ 1.15 (d, J = 6.9 Hz, 12 H, CH(CH_3)$_2$), 2.20 (s, 3 H, C(N-Ar)CH_3), 2.64−2.77 (m, 2 H, C*H*(CH$_3$)$_2$), 7.06−7.20 (m, 3 H, CH), 7.59 (dd, J = 8.0, 1.3 Hz, 1 H, CH), 7.65−7.72 (m, 1 H, CH), 8.33 (dd, J = 7.5, 1.3 Hz, 1 H, CH). $^{13}C\{^1H\}$ NMR ($CDCl_3$): δ 17.98 (1 C, C(N-Ar)*C*H_3), 23.55 (2 C, CH(*C*H_3)(CH$_3$)), 23.90 (2 C, CH(CH$_3$)(*C*H_3)), 28.97 (2 C, *C*H(CH$_3$)(CH$_3$)), 120.73 (1 C, CH), 123.72 (2 C, CH), 124.43 (1 C, CH), 129.89 (1 C, CH), 136.34 (2 C, C), 139.46 (1 C, CH), 141.68 (1 C, CH), 146.80 (1 C, C), 158.09 (1 C, C), 166.62 (1 C, *C*(N-Ar)CH$_3$). Anal. Calcd for $C_{19}H_{23}BrN_2$ (359.31): C, 63.51; H, 6.45; N, 7.80. Found: C, 63.48; H, 6.31; N, 7.99.

Synthesis of (Thiophen-3-yl)trimethylstannane. A solution of 3-bromothiophene (0.937 mL, 10.0 mmol) in 35 mL of Et_2O was cooled to −78 °C and treated dropwise with a 1.6 M solution of *n*-BuLi in hexanes (12.5 mL, 20.0 mmol). The reaction mixture was stirred at that temperature for 30 min, and then a solution of Me_3SnCl (2.99 g, 15.0 mmol) in Et_2O (15 mL) was added dropwise within 10 min. The mixture was allowed to stand at −78 °C for 1 h and then was slowly warmed to −35 °C and quenched with 30 mL of a saturated $NaHCO_3$ aqueous solution. The aqueous phase was extracted with 3 × 25 mL of Et_2O. The combined organic layers were dried over Na_2SO_4. Removal of the solvent under reduced pressure gave the stannane product as a crude orange oil. The product was purified by fractional distillation under reduced pressure (1.0 × 10^{-2} mmHg, 50−55 °C) to afford a colorless oil (yield 50%). ^1H NMR ($CDCl_3$): δ 0.32 (s, 9 H, CH_3), 7.20 (dd, J = 4.6, 1.0 Hz, 1 H, CH), 7.39 (dd, J = 2.5, 1.0 Hz, 1 H, CH), 7.46 (dd, J = 4.6, 2.5 Hz, 1 H, CH). $^{13}C\{^1H\}$ NMR ($CDCl_3$): δ 5.05 (3 C, CH_3), 125.98 (1 C, CH), 132.05 (1 C, CH), 133.37 (1 C, CH), 139.29 (1 C, C). Anal. Calcd for $C_7H_{12}SSn$ (246.92): C, 34.05; H, 4.90. Found: C, 33.96; H, 4.88.

Synthesis of (Benzo[*b*]thiophen-3-yl)trimethylstannane. A solution of 3-bromothianaphthene (5.0 mmol) in 20 mL of Et_2O was cooled to −78 °C and treated dropwise with a 1.6 M solution of *n*-BuLi in hexanes (6.9 mL, 11.0 mmol). The reaction mixture was stirred at that temperature for 30 min, and then a solution of Me_3SnCl (2.19 g, 11.0 mmol) in Et_2O (15 mL) was added dropwise within 10 min. The mixture was allowed to stand at −78 °C for 1 h and then was slowly warmed to −35 °C and quenched with 30 mL of a saturated $NaHCO_3$ aqueous solution. The aqueous phase was extracted with 3 × 15 mL of Et_2O. The combined organic layers were dried over Na_2SO_4. Removal of the solvent under reduced pressure gave the stannane product as a colorless oil (yield 54%). ^1H NMR ($CDCl_3$): δ 0.43 (s, 9 H, CH_3), 7.31−7.40 (m, 2 H, CH), 7.45 (s, 1 H, CH), 7.80 (m, 1 H, CH), 7.98 (m, 1 H, CH). $^{13}C\{^1H\}$ NMR ($CDCl_3$): δ 5.01 (3 C, CH_3), 123.34 (2 C, CH), 124.37 (1 C, CH), 124.58 (1 C, CH), 125.53 (1 C, C), 125.61 (1 C, C), 133.07 (1 C, CH), 137.35 (1 C, C). Anal. Calcd for $C_{11}H_{14}SSn$ (296.98): C, 44.48; H, 4.75. Found: C, 44.38; H, 4.70.

Synthesis of [1-(6-thiophen-3-ylpyridin-2-yl)ethylidene](2,6-diisopropylphenyl)amine (N_2^{3Th}). A solution of N_2^{Br} (0.300 g, 0.84 mmol) and (thiophen-3-yl)trimethylstannane (0.309 g, 1.252 mmol) in 3 mL of toluene was treated with a solution of $Pd(dba)_2$ (0.014 g, 0.025 mmol) and PPh_3 (0.042 g, 0.162 mmol) in toluene (1 mL). The reaction mixture was refluxed for 20 h, and then cooled to room temperature and treated with water (10 mL). The formed layers were separated, and the organic phase was washed with 2 × 20 mL of water and then dried over Na_2SO_4. The collected organic layers were evaporated under reduced pressure, and the crude product was purified via flash chromatography on neutral alumina (*n*-pentane:Et_2O = 97.5:2.5) to afford a pale yellow crystalline product (yield 63%). IR (KBr): ν 1645 cm^{-1} (C═N). ^1H NMR ($CDCl_3$): δ 1.33 (s, 6 H, CH(CH_3)(CH$_3$)), 1.35 (s, 6 H CH(CH$_3$)(CH_3)), 2.46 (s, 3 H, N═CCH_3), 2.96 (m, 2 H, C*H*(CH$_3$)(CH$_3$)), 7.26−7.37 (m, 3 H, CH), 7.58−7.62 (m, 1 H, CH), 7.88−7.96 (m, 2 H, CH), 8.01 (t, J = 7.6 Hz, 1 H, CH), 8.18 (m, 1 H, CH), 8.43 (d, J = 7.6 Hz, 1 H, CH). $^{13}C\{^1H\}$ NMR ($CDCl_3$): δ 17.52 (1 C, N═C*C*H$_3$), 23.20 (2 C, CH(*C*H$_3$)(CH$_3$)), 23.52 (2 C, CH(CH$_3$)(*C*H$_3$)), 28.56 (2 C, *C*H(CH$_3$)(CH$_3$)), 119.52 (1 C, CH), 121.24 (1 C, CH), 123.29 (1 C, CH), 123.80 (1 C, CH), 123.89 (1 C, CH), 126.57 (1 C, CH), 126.65 (1 C, CH), 136.13 (1 C, CH), 137.48 (1 C, CH), 141.87 (1 C, C), 142.51 (1 C, C), 146.88 (1 C, C), 152.57 (1 C, C), 156.38 (1 C, C), 167.53 (N═*C*CH$_3$). Anal. Calcd for $C_{23}H_{26}N_2S$ (362.53): C, 76.20; H, 7.23; N, 7.73. Found: C, 76.28; H, 7.34; N, 7.82.

Synthesis of [1-(6-(Benzo[*b*]thiophen-3-yl)pyridin-2-yl)ethylidene](2,6-diisopropylphenyl)amine (N_2^{3BT}). A solution of N_2^{Br} (0.300 g, 0.84 mmol) and (benzo[*b*]thiophen-3-yl)trimethylstannane (0.297 g, 1.00 mmol) in 3 mL of toluene was treated with a solution of $Pd(dba)_2$ (0.014 g, 0.025 mmol) and PPh_3 (0.044 g, 0.167 mmol) in toluene (1 mL). The reaction mixture was refluxed for 70 h and then cooled to room temperature and treated with water (10 mL). The formed layers were separated, and the organic phase was washed with 2 × 20 mL of water and then dried over Na_2SO_4. The collected organic layers were evaporated under reduced pressure, and the crude product was purified via flash chromatography on neutral alumina (*n*-pentane:Et_2O = 95:5) to afford a pale yellow crystalline product (yield 84%). IR (KBr): ν 1642 cm^{-1} (C═N). ^1H NMR ($CDCl_3$): δ 1.17 (s, 6 H, CH(CH_3)(CH$_3$)), 1.20 (s, 6 H CH(CH$_3$)(CH_3)), 2.34 (s, 3 H, N═CCH$_3$), 2.81 (m, 2 H, C*H*(CH$_3$)(CH$_3$)), 7.08−7.23 (m, 3 H, CH), 7.37−7.53 (m, 2 H, CH), 7.80−7.97 (m, 4 H, CH), 8.37 (dd, J = 7.59, 1.2 Hz, 1 H, CH), 8.68 (m, 1 H, CH). $^{13}C\{^1H\}$ NMR ($CDCl_3$): δ 18.22 (1 C, N═C*C*H$_3$), 23.60 (2 C, CH(*C*H$_3$)(CH$_3$)), 23.93 (2 C, CH(CH$_3$)(*C*H$_3$)), 29.00 (2 C, *C*H(CH$_3$)(CH$_3$)), 120.20 (1 C, CH), 123.49 (1 C, CH), 123.71 (1 C, CH), 124.07 (2 C, CH), 124.29 (1 C, CH), 125.12 (1 C, CH), 125.35 (2 C, CH), 127.40 (1 C, CH), 136.54 (1 C, C), 137.08 (1 C, C), 137.90 (1 C, CH), 139.70 (1 C, C), 141.74 (2 C, C), 147.16 (1 C, C), 154.26 (1 C, C) 156.80 (1 C, C), 167.93 (1 C, N═*C*CH$_3$). Anal. Calcd for $C_{27}H_{28}N_2S$ (412.59): C, 78.60; H, 6.84; N, 6.79. Found: C, 78.49; H, 6.66; N, 6.63.

Synthesis of 2-(Tri-*n*-butylstannanyl)pyridine. To a stirred solution of 2-bromopyridine (3.0 mL, 4.98 g, 31.5 mmol) in 150 mL of Et_2O at −78 °C was added 12.6 mL (31.5 mmol) of a 1.6

M solution of *n*-BuLi in hexanes over 10 min. After 30 min, *n*-Bu_3SnCl (9.0 mL, 10.8 g, 31.8 mmol) was added portionwise and stirring was continued for 2 h. The resulting mixture was warmed to room temperature and then treated with 60 mL of a saturated NH_4Cl aqueous solution. The organic layer was washed with 2 × 50 mL of water. The aqueous layer was extracted with 3 × 30 mL of Et_2O, and the combined organic layers were dried over Na_2SO_4. Evaporation under reduced pressure of the solvent gave the product as a pale orange oil (yield 93%). ^{1}H NMR ($CDCl_3$): δ 0.85 (t, J = 7.3 Hz, 9H, CH_3), 1.00−1.20 (m, 6H, CH_2), 1.26−1.35 (m, 6H, CH_2), 1.42−1.66 (m, 6H, CH_2), 7.08 (ddd, J = 6.4, 4.9, 1.5 Hz, 1H, CH), 7.37 (ddd, J = 7.5, 1.5, 1.0 Hz, 1H, CH), 7.46 (ddd, J = 7.5, 7.5, 1.9 Hz, 1H, CH), 8.71 (ddd, J = 2.9, 1.9, 1.0 Hz, 1H, CH). ^{13}C{^{1}H} NMR ($CDCl_3$): δ 10.41 (3C, Sn−CH_2), 14.30 (3C, CH_3), 27.98 (3C, CH_2), 29.72 (3C, CH_2), 122.60 (1C, CH), 132.97 (1C, CH), 133.86 (1C, CH), 151.13 (1C, CH), 174.70 (1C, C). Anal. Calcd for $C_{17}H_{31}NSn$ (368.14): C, 55.46; H, 8.49; N, 3.80. Found: C, 55.36; H, 8.60; N, 3.77.

Synthesis of 2-Methyl-6-(trimethylstannanyl)pyridine. To a stirred solution of 2-bromo-6-methylpyridine (1.71 mL, 2.586 g, 15.0 mmol) in 60 mL of THF at −78 °C was added 9.9 mL (15.8 mmol) of a 1.6 M solution of *n*-BuLi in hexanes over a period of 2 h. After 30 min, Me_3SnCl (3.29 g, 16.5 mol) was added portionwise and stirring was continued for 1 h. The resulting mixture was warmed to room temperature (ca. 20 min) and then treated with 60 mL of a saturated $NaHCO_3$ aqueous solution. The organic layer was washed with 2 × 30 mL of the saturated $NaHCO_3$ solution and then 2 × 30 mL of water. The aqueous layer was extracted with 3 × 30 mL of Et_2O. The organic layers were combined and dried over Na_2SO_4. Removal of the solvent under reduced pressure gave the product as a pale orange oil (yield 97%). ^{1}H NMR ($CDCl_3$): δ 0.35 (s, 9H, $Sn(CH_3)_3$), 2.57 (s, 3H, Ar−CH_3), 6.98 (d, J = 7.7 Hz, 1H, CH), 7.25 (d, J = 7.2 Hz, 1H, CH), 7.26−7.39 (m, 1H, CH). ^{13}C{^{1}H} NMR ($CDCl_3$): δ −7.68 (3C, $Sn(CH_3)_3$), 25.55 (1C, Ar−CH_3), 122.56 (1C, CH), 129.33 (1C, CH), 134.30 (1C, CH), 159.39 (1C, C), 173.16 (1C, C). Anal. Calcd for $C_9H_{15}NSn$ (255.91): C, 42.24; H, 5.91; N, 5.47. Found: C, 42.13; H, 6.04; N, 5.39.

Synthesis of 1-(6′-Methyl[2,2′]bipyridin-6-yl)ethanone. A deaerated solution of 2-methyl-6-(trimethylstannanyl)pyridine (1.60 g, 6.25 mmol) and 1-(6-bromopyridin-2-yl)ethanone (1.25 g, 6.25 mmol) in 18 mL of toluene was treated with a solution of $Pd(dba)_2$ (0.073 g, 0.13 mmol) and PPh_3 (0.236 g, 0.91 mmol) in toluene (2 mL). The reaction mixture was refluxed for 16 h, cooled to room temperature, and then treated with 50 mL of saturated aqueous $NaHCO_3$. The organic layer was separated, washed with 2 × 30 mL of a saturated $NaHCO_3$ solution, 2 × 30 mL of water, and 2 × 50 mL of brine, and dried over Na_2SO_4. Upon concentration of the resulting solution to dryness under reduced pressure the product was obtained in 93% yield. Mp: 85−87 °C. IR (KBr): ν 1693 cm^{-1} (C═O). ^{1}H NMR ($CDCl_3$): δ 2.65 (s, 3H, py−CH_3), 2.84 (s, 3H, C(O)CH_3), 7.22 (ddd, J = 7.7, 1.0, 0.6 Hz, 1H, CH), 7.71−7.79 (m, 1H, CH), 7.90−7.98 (m, 1H, CH), 8.05 (dd, J = 7.8, 1.4 Hz, 1H, CH), 8.33 (ddd, J = 7.8, 1.0, 0.6 Hz, 1H, CH), 8.66 (dd, J = 7.6, 1.4 Hz, 1H, CH). ^{13}C{^{1}H} NMR ($CDCl_3$): δ 25.29 (1C, CH_3), 26.42 (1C, CH_3), 118.77 (1C, CH), 121.91 (1C, CH), 124.35 (1C, CH), 124.99 (1C, CH), 137.79 (1C, CH), 138.72 (1C, CH), 153.57 (1C, C), 156.38 (1C, C), 156.56 (1C, C), 158.72 (1C, C), 201.10 (1C, *C*(O)CH_3). Anal. Calcd for $C_{13}H_{12}N_2O$ (212.25): C, 73.57; H, 5.70; N, 13.20. Found: C, 73.68; H, 5.59; N, 13.31.

Synthesis of [1-([2,2′]Bipyridin-6-yl)ethylidene](2,6-diisopropylphenyl)amine (N_2^{Py}). A solution of N_2^{Br} (0.57 g, 1.59 mmol) and 2-(tri-*n*-butylstannanyl)pyridine (0.247 g, 1.67 mmol) in 15 mL of toluene was treated with $Pd(PPh_3)_4$ (0.055 g, 0.048 mmol) and refluxed for 18 h. The reaction mixture was cooled to room temperature, and the solvent was removed under reduced pressure to give the product as a yellow solid, which was washed with cold MeOH (yield 88%). Mp: 186 °C. IR (KBr): ν 1640 cm^{-1} (C═N). ^{1}H NMR ($CDCl_3$): δ 1.18 (d, J = 6.8 Hz, 12H, $CH(CH_3)_2$), 2.35 (s, 3H, py−C(NR)CH_3), 2.81 (sept, J = 6.8 Hz, 2H, $CH(CH_3)_2$), 7.09−7.23 (m, 3H, CH), 7.34 (ddd, J = 7.5, 4.8, 1.2 Hz, 1H, CH), 7.85 (td, J = 7.8, 1.8 Hz, 1H, CH), 7.96 (t, J = 7.9 Hz, 1H, CH), 8.42 (dd, J = 7.9, 1.0 Hz, 1H, CH), 8.55 (dd, J = 7.9, 1.1 Hz, 1H, CH), 8.57 (dt, J = 8.0, 1.0 Hz, 1H, CH), 8.72 (ddd, J = 4.9, 0.2, 0.1 Hz, 1H, CH). ^{13}C{^{1}H} NMR ($CDCl_3$): δ 17.93 (1C, C(N-R)-CH_3), 23.60 (2C, $CH(CH_3)(CH_3)$), 23.91 (2C, $CH(CH_3)(CH_3)$), 28.95 (2C, $CH(CH_3)(CH_3)$), 121.77 (1C, CH), 121.87 (1C, CH), 122.61 (1C, CH),123.67 (2C, CH), 124.21 (1C, CH),124.50 (1C, CH), 136.51 (2C, C), 137.58 (1C, CH), 138.10 (1C, CH), 147.21 (1C, C), 149.86 (1C, C), 155.86 (1C, C), 156.32 (1C, C), 156.71 (1C, C), 167.74 (1C, *C*(N−R)CH_3). Anal. Calcd for $C_{24}H_{27}N_3$ (357.49): C, 80.63; H, 7.61; N, 11.75. Found: C, 80.50; H, 7.56; N, 11.83.

Synthesis of [1-(6′-Methyl[2,2′]bipyridin-6-yl)ethylidene](2,6-diisopropylphenyl)amine (N_2^{PyMe}). A solution of 1-(6′-methyl-[2,2′]bipyridin-6-yl)ethanone (0.424 g, 2.00 mmol) and 2,6-diisopropylaniline (1.68 mL, 8.00 mmol) in 20 mL of MeOH was refluxed for 24 h. The resulting mixture was concentrated to ca. 8−10 mL and cooled to −24 °C. After 2 h, yellow crystals of N_2^{PyMe} (0.41 g, 1.10 mmol, 55%) were collected by filtration. A second crop (0.18 g, 0.48 mmol) was obtained from the mother liquor maintained at −24 °C for 24 h (overall yield: 80%). Mp: 150−152 °C. IR (KBr): ν 1638 cm^{-1} (C═N). ^{1}H NMR ($CDCl_3$): δ 1.17 (d, J = 6.9 Hz, 12H, $CH(CH_3)_2$), 2.33 (s, 3H, py−C(N-R)-CH_3), 2.67 (s, 3H, py−CH_3), 2.79 (sept, J = 6.9 Hz, 2H, $CH(CH_3)_2$), 7.04−7.23 (m, 4H, CH), 7.70−7.77 (m, 1H, CH), 7.90−7.98 (m, 1H, CH), 8.35 (ddd, J = 7.7, 0.9, 0.6 Hz, 1H, CH), 8.39 (dd, J = 7.8, 1.2 Hz, 1H, CH), 8.57 (dd, J = 7.8, 1.2 Hz, 1H, CH). ^{13}C{^{1}H} NMR ($CDCl_3$): δ 17.93 (1C, py-CH_3), 23.60 (2C, $CH(CH_3)(CH_3)$), 23.90 (2C, $CH(CH_3)(CH_3)$), 25.36 (1C, C(N-R)-CH_3), 28.92 (2C, $CH(CH_3)(CH_3)$), 118.71 (1C, CH), 121.64 (1C, CH), 122.62 (1C, CH), 123.64 (2C, CH), 124.04 (1C, CH),124.16 (1C, CH), 136.52 (2C, C), 137.70 (1C, CH), 137.98 (1C, CH), 147.23 (1C, C), 155.84 (1C, C), 156.10 (1C, C), 156.23 (1C, C), 158.60 (1C, C), 167.86 (1C, *C*(N-Ar)CH_3). Anal. Calcd for $C_{25}H_{29}N_3$ (371.53): C, 80.82; H, 7.87; N, 11.31. Found: C, 80.65; H, 7.74; N, 11.21.

General Procedure for the Syntheses of the Co^{II} Catalyst Precursors. To the blue solution of anhydrous $CoCl_2$ (0.18 mmol) in THF (3 mL) the appropriate ligand (0.20 mmol) was added in one portion. The resulting green mixture was stirred at room temperature for 3 h. During that time a precipitate formed, which was decanted, transferred onto a sintered-glass frit, washed with Et_2O, and dried under a stream of nitrogen.

[(1-(6-Bromopyridin-2-yl)ethylidene)(2,6-diisopropylphenyl)-amine]cobalt(II) Dichloride ($CoCl_2N_2^{Br}$). This compound was obtained as green microcrystals (yield 91%). IR (KBr): ν 1589 cm^{-1} (C═N). μ_{eff}: 4.71 μ_B (25 °C). Electronic spectra: diffuse reflectance, 370 sh, 573, 631, 668, 1000, 1398, 1681 nm; CH_2Cl_2 solution, 362 sh, 571 (ϵ = 750), 632 (ϵ 1030), 676 (ϵ = 1680), 1005 (ϵ = 130), 1386 nm (ϵ = 390). Anal. Calcd for $C_{19}H_{23}BrCl_2CoN_2$ (489.15) C, 46.65; H, 4.74; N, 5.73. Found: C, 46.50; H, 4.71; N, 5.68.

[(1-(6-(Thiophen-3-yl)pyridin-2-yl)ethylidene)(2,6-diisopropylphenyl)amine]cobalt(II) Dichloride ($CoCl_2N_2^{3Th}$). This compound was obtained as green microcrystals (yield 92%). IR (KBr): ν 1580 cm^{-1} (C═N). μ_{eff}: 4.68 μ_B (25 °C). Electronic spectra: diffuse reflectance, 377, 452 sh, 560, 633 sh, 668, 1020, 1334, 1647 nm; CH_2Cl_2 solution, 373 (ϵ = 8000), 562 (ϵ = 1400), 671 (ϵ = 2700), 998 (ϵ = 100), 1351 nm (ϵ = 380). Anal. Calcd for $C_{23}H_{26}Cl_2CoN_2S$: C, 56.11; H, 5.32; N, 5.69. Found: C, 56.19; H, 5.29; N, 5.57.

[(1-(6-(Benzo[*b*]thiophen-3-yl)pyridin-2-yl)ethylidene)(2,6-diisopropylphenyl)amine]cobalt(II) Dichloride ($CoCl_2N_2^{3BT}$). This

Scheme 3

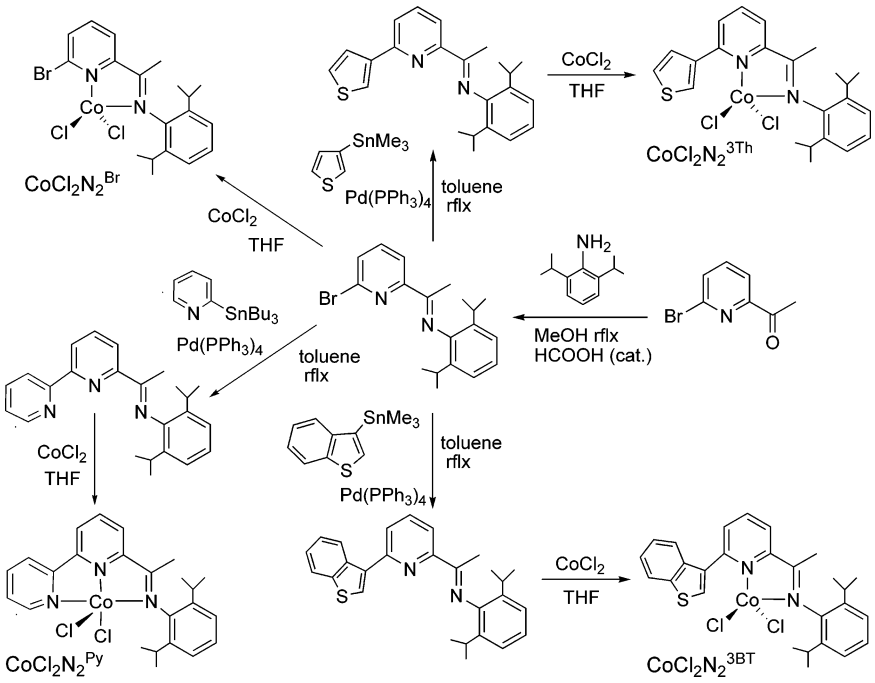

compound was obtained as green microcrystals (yield 87%). IR (KBr): ν 1590 cm^{-1} (C═N). μ_{eff}: 4.69 μ_B (25 °C). Electronic spectra: diffuse reflectance, 381, 452 sh, 559, 623 sh, 667, 1015, 1333, 1642 nm; CH_2Cl_2 solution, 379 (ϵ = 11 000), 568 (ϵ = 1400), 665 (ϵ = 2600), 1002 (ϵ = 110), 1370 nm (ϵ = 390). Anal. Calcd for $C_{27}H_{28}Cl_2CoN_2S$: C, 59.78; H, 5.20; N, 5.16. Found: C, 59.60; H, 5.09; N, 4.99.

[(1-([2,2′]Bipyridin-6-yl)ethylidene)(2,6-diisopropylphenyl)-amine]cobalt(II) Dichloride ($CoCl_2N_2^{Py}$). This compound was obtained as a pale green powder (yield 88%). IR (KBr): ν 1585 cm^{-1} (C═N). μ_{eff}: 4.75 μ_B (25 °C). Electronic spectra: diffuse reflectance, 375 sh, 595, 650, 919, 1220, 1790 nm; CH_2Cl_2 solution, 380 sh, 590 (ϵ = 92), 645 (ϵ = 105), 920 (ϵ = 20), 1230 nm (ϵ = 22). Anal. Calcd for $C_{24}H_{27}Cl_2CoN_3$ (487.33): C, 59,15; H, 5,58; N, 8,62. Found: C, 59.03; H, 5.47; N, 8.60.

[(1-(6′-Methyl[2,2′]bipyridin-6-yl)ethylidene)(2,6-diisopropy-lphenyl)amine]cobalt(II) Dichloride ($CoCl_2N_2^{PyMe}$). This compound was obtained as a pale green powder (yield 97%). IR (KBr): ν 1593 cm^{-1} (C═N). μ_{eff}: 4.80 μ_B (25 °C). Electronic spectra: diffuse reflectance, 365 sh, 588, 641, 909, 1219, 1786 nm; CH_2Cl_2 solution, 370 sh, 585 (ϵ = 90), 641 (ϵ = 100), 917 (ϵ = 15), 1220 nm (ϵ = 18). Anal. Calcd for $C_{25}H_{29}Cl_2CoN_3$ (501.31): C, 59.89; H, 5.83; N, 8.38. Found: C, 59.81; H, 5.71; N, 8.40.

General Procedure for Ethylene Oligomerization. A 500 mL stainless steel reactor was heated to 60 °C under vacuum overnight and then cooled to room temperature under a nitrogen atmosphere. A MAO solution, prepared by diluting 1.5 mL of a stock toluene solution of MAO (2.5 mmol) with toluene (93.5 mL), was introduced by suction into the reactor, previously evacuated by a vacuum pump. The system was pressurized with ethylene to 5 bar and stirred for 5 min. Afterward, the ethylene pressure was released slowly and 5 mL of a precatalyst solution, prepared by dissolving the solid precatalyst (12 μmol) in 50 mL of toluene, was syringed into the reactor. The system was repressurized to 5 bar and stirred at 1500 rpm. Ethylene was continuously fed to maintain the reactor pressure at the desired value. The temperature inside the reactor increased solely from the exothermicity of the reaction and reached a maximum value within 5−7 min. After 30 min, the reaction was stopped by cooling the reactor to −20 °C, depressurizing, and introducing 2 mL of acidic MeOH (5% HCl). Depending on the oligomerization products, two different procedures were followed. For reactions yielding mixtures of α-olefins, *n*-heptane was injected into the reactor as the GC internal standard and the reactor contents were stirred for 10 min. The solution was analyzed by GC and GC-MS. The moles of the C6 and C8 fractions were determined by GC using calibration curves with standard toluene solutions containing concentrations of 1-hexene and 1-octene as close as possible to those in the sample under analysis. Schulz−Flory α constants were determined by the molar ratio of the couple C8/C6. The moles of C4 were calculated by the Schulz−Flory α constant and the moles of C6 by the formula moles of C4 = (moles of C6)/α, whereas the moles of the oligomers in the C10−C20 range were calculated by the Schulz−Flory α constant and the moles of C8 by the formula moles of Ci = (moles of C8)$\alpha^{i-8/2}$. The total moles of converted ethylene was obtained by the formula moles of C_2H_4 = $\sum$(moles of Ci)(i/2) with i = 4−20; therefore, the TOFs were obtained. For reactions yielding exclusively butenes, the reactor contents, after being cooled to −50 °C, were transferred into a flask immersed in a bath at −50 °C. Oligomers were distilled over a Vigreux column (70 °C), condensed into a cooling trap (−196 °C) containing isobutane as the GC internal standard, and analyzed by GC.

EPR Study of the Activation of the Dichloride Precursors by MAO. The activation of the dichloride precursors was studied by X-band EPR spectroscopy, using the following procedures.

(a) In Situ Study. The appropriate Co^{II} complex was suspended in toluene in a Schlenk tube inside a glovebox (partial dissolution with formation of a green solution was observed only for $CoCl_2N_2^{2ThE}$). An excess of solid MAO (30 equiv) was added, and a brownish solution was obtained, which was poured into an EPR tube. This was immediately sealed and frozen by means of a liquid nitrogen bath. The tube was introduced into the EPR probe, which was precooled to 5 K. Spectra were acquired in the temperature range 5−293 K. Thermal cycles from 293 to 5 K were repeated three times to check the stability of the products.

(b) Operando Study. A toluene suspension of the appropriate Co^{II} complex in an EPR tube, cooled to 223 K, was saturated with ethylene. After the addition of solid MAO (30 equiv), the solution was warmed to 293 K and then the tube was immersed into a liquid nitrogen bath. The acquisition of the EPR spectra was carried out as described above.

Scheme 4

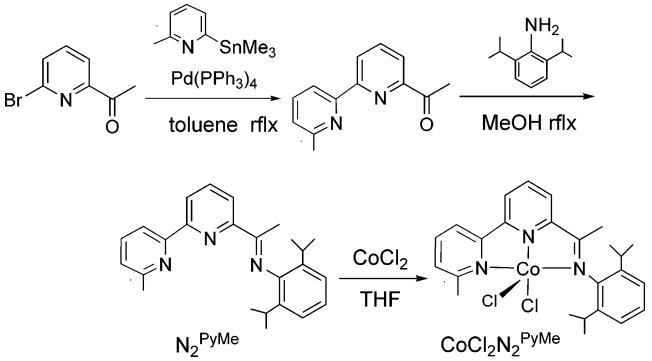

Reactions of $CoCl_2N_2^{Ph}$ and $CoCl_2N_2^{2Th}$ with MAO. Procedure A. A 250 mL Schlenk flask equipped with a magnetic stirrer bar was flamed under vacuum and cooled to room temperature under an argon atmosphere. A MAO solution, prepared by diluting 1.5 mL of a stock toluene solution of MAO (2.5 mmol, 200 equiv) with toluene (93.5 mL), was transferred by cannula into the flask. The solid precatalyst (12 μmol) suspended in 5 mL of toluene was syringed into the flask. The system was stirred for either 10 or 30 min and then treated with 10 mL of acidic MeOH (5% HCl). The organic layer was separated from the aqueous phase, dried over Na_2SO_4, and evaporated under reduced pressure to give a yellow pale solid that was authenticated as the intact (imino)pyridine ligand by ^{1}H NMR spectroscopy.

Procedure B (EPR Conditions). A 25 mL Schlenk flask equipped with a magnetic stirrer bar was flamed under vacuum and cooled to room temperature under an argon atmosphere. The solid precatalyst (61 μmol) was suspended in 2 mL of toluene into the flask. A stock toluene solution of MAO (1.1 mL, 30 equiv, 1.83 mmol) was transferred by cannula into the flask. The system was stirred for 1 min and then treated with 5 mL of acidic MeOH (5% HCl). The organic layer was separated from the aqueous phase, dried over Na_2SO_4, and evaporated under reduced pressure to give a yellow pale solid that was authenticated as the intact (imino)-pyridine ligand by ^{1}H NMR spectroscopy.

DFT Modeling Study. All of the model structures were calculated with the unrestricted B3LYP hybrid density functional method[12,13] using the Gaussian 03 program package (Revision C.02).[14] The basis set for the cobalt atom was provided by the effective core potential of Hay and Wadt[15] with the associated double-ζ basis set. For the other atoms, the 6-31G(d,p) basis set was used. The nature of the optimized point was established by calculating the vibrational frequencies. In all of the models, the imino methyl group and the isopropyl phenyl substituents of the ligands were replaced by hydrogen atoms. A test calculation with all the atoms for $[Co(CH_3)N_2^{2Th}]^+$ showed that the approximations used did not influence the coordination geometry around the cobalt atom as well as the electronic state and the total spin density. The Cartesian coordinates of the complex cations $[Co(CH_3)N_2^{2Th}]^+$, $[Co(CH_3)N_2^{Ph}]^+$, $[Co(CH_3)N_2^{3Th}]^+$, and $[Co(CH_3)N_2^{Py}]^+$ are available in the Supporting Information.

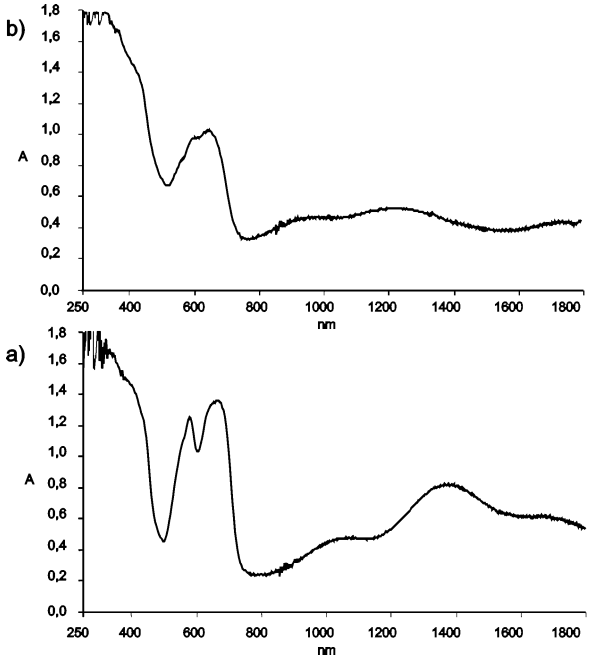

Figure 1. Diffuse reflectance spectra of (a) $CoCl_2N_2^{Ph}$ and (b) $CoCl_2N_2^{Py}$.

Results

Synthesis and Characterization of the (Imino)pyridine Co^{II} Complexes $CoCl_2N_2^{3Th}$ and $CoCl_2N_2^{3BT}$. The new (imino)pyridine ligands N_2^{3Th} and N_2^{3BT} were isolated as pale yellow crystals by Stille coupling between N_2^{Br} and (thiophen-3-yl)-trimethylstannane or (benzo[*b*]thiophen-3-yl)trimethylstannane, respectively. The corresponding Co^{II} complexes $CoCl_2N_2^{3Th}$ and $CoCl_2N_2^{3BT}$ as well as the N_2^{Br} derivative $CoCl_2N_2^{Br}$ were straightforwardly obtained as green crystals in high yield by reacting 1 equiv of the ligand with anhydrous $CoCl_2$ in THF (Scheme 3).

All complexes are high spin in the solid state with μ_{eff} values of about 4.7 μ_B at room temperature, which is typical for a d^7 metal ion in a tetrahedral coordination geometry.[1,2] Notice that a distorted-tetrahedral geometry has been previously determined by X-ray methods for both $CoCl_2N_2^{2ThE}$ and $CoCl_2N_2^{Ph}$.[1] Consistent with a tetrahedral geometry, the electronic spectra of the present Co^{II} complexes, both in solution and in the solid state, showed three d−d absorption bands in the spectral regions 1800−1640, 1430−1330, and 1050−990 nm, respectively, and three or two higher intensity bands in the region 690−550 nm.[1,2]

Due to the fast spin−lattice relaxation times of the quartet spin state, $CoCl_2N_2^{3Th}$, $CoCl_2N_2^{3BT}$, and $CoCl_2N_2^{Br}$ were EPR silent at room temperature both in the solid state and in CH_2Cl_2 solution.[16] Only at very low temperature (10 K) were EPR signals typical of high-spin tetrahedral Co^{II} species observed (see the Supporting Information for details). As previously observed for the thien-2-yl regioisomer $CoCl_2N_2^{2ThE}$ and the

(12) Becke, A. D. *J. Chem. Phys.* **1993**, *98*, 5648.
(13) Lee, C.; Yang, W.; Parr, R. G. *Phys. Rev. B* **1988**, *37*, 785.
(14) Frisch, M. J.; Trucks, G. W.; Schlegel, H. B.; Scuseria, G. E.; Robb, M. A.; Cheeseman, J. R.; Montgomery, J. A., Jr.; Vreven, T.; Kudin, K. N.; Burant, J. C.; Millam, J. M.; Iyengar, S. S.; Tomasi, J.; Barone, V.; Mennucci, B.; Cossi, M.; Scalmani, G.; Rega, N.; Petersson, G. A.; Nakatsuji, H.; Hada, M.; Ehara, M.; Toyota, K.; Fukuda, R.; Hasegawa, J.; Ishida, M.; Nakajima, T.; Honda, Y.; Kitao, O.; Nakai, H.; Klene, M.; Li, X.; Knox, J. E.; Hratchian, H. P.; Cross, J. B.; Bakken, V.; Adamo, C.; Jaramillo, J.; Gomperts, R.; Stratmann, R. E.; Yazyev, O.; Austin, A. J.; Cammi, R.; Pomelli, C.; Ochterski, J. W.; Ayala, P. Y.; Morokuma, K.; Voth, G. A.; Salvador, P.; Dannenberg, J. J.; Zakrzewski, V. G.; Dapprich, S.; Daniels, A. D.; Strain, M. C.; Farkas, O.; Malick, D. K.; Rabuck, A. D.; Raghavachari, K.; Foresman, J. B.; Ortiz, J. V.; Cui, Q.; Baboul, A. G.; Clifford, S.; Cioslowski, J.; Stefanov, B. B.; Liu, G.; Liashenko, A.; Piskorz, P.; Komaromi, I.; Martin, R. L.; Fox, D. J.; Keith, T.; Al-Laham, M. A.; Peng, C. Y.; Nanayakkara, A.; Challacombe, M.; Gill, P. M. W.; Johnson, B.; Chen, W.; Wong, M. W.; Gonzalez, C.; Pople, J. A. *Gaussian 03*, revision C.02; Gaussian, Inc.: Wallingford, CT, 2004.
(15) Hay, P. J.; Wadt, W. R. *J. Chem. Phys.* **1985**, *82*, 299.
(16) (a) Bencini, A.; Gatteschi, D. In *Transition Metal Chemistry*; Figgis, B. N., Melson, G., Eds.; Marcel Dekker: New York, 1982; Vol. 8. (b) Pilbrow, J. R. *Transition Ion Electron Paramagnetic Resonance*; Clarendon Press: Oxford, U.K., 1990.

Table 1. Ethylene Oligomerization with Cobalt(II) 6-(Organyl)-2-(imino)pyridine Dichloride Catalyst Precursors[a]

			alkene			amt (mol %)				
entry	cat. precursor	ΔT (°C)	TOF[b,c]	productivity[b,d]	α[b,e]	C4	C6	C8	C10−14	α-olefin selectivity[b] (%)
1	$CoCl_2N_2^{2Th}$	12	665000	3724	0.08	92.0	7.4	0.6	<0.1	90
2	$CoCl_2N_2^{3Th}$	4	113000	633	*f*					92
3	$CoCl_2N_2^{2ThE}$	9	407000	2279	0.10	90.0	9.0	0.9	0.1	93
4	$CoCl_2N_2^{2BT}$	20	927000	5191	0.20	80.0	16.0	3.2	0.8	91
5	$CoCl_2N_2^{3BT}$	4	115000	644	*f*					93
6	$CoCl_2N_2^{Ph}$	6	183000	1025	*f*					92

[a] Reaction conditions: catalyst precursor, 1.2 μmol; MAO equiv, 2100; C_2H_4 pressure, 5 bar; toluene, 100 mL; initial temperature, 23 °C; reaction time, 30 min. [b] Determined by GC. [c] In units of mol of C_2H_4 converted (mol of Co)$^{-1}$ h^{-1}. [d] In units of g of C_2H_4 converted (mmol of Co)$^{-1}$ h^{-1} bar^{-1}. [e] Schulz-Flory parameter, α = rate of propagation (rate of propagation + rate of chain transfer)$^{-1}$ = mol of C_{n+2} (mol of C_n)$^{-1}$. [f] Not determined. Almost exclusively butenes produced, with prevalent *E* configuration for 2-butene.

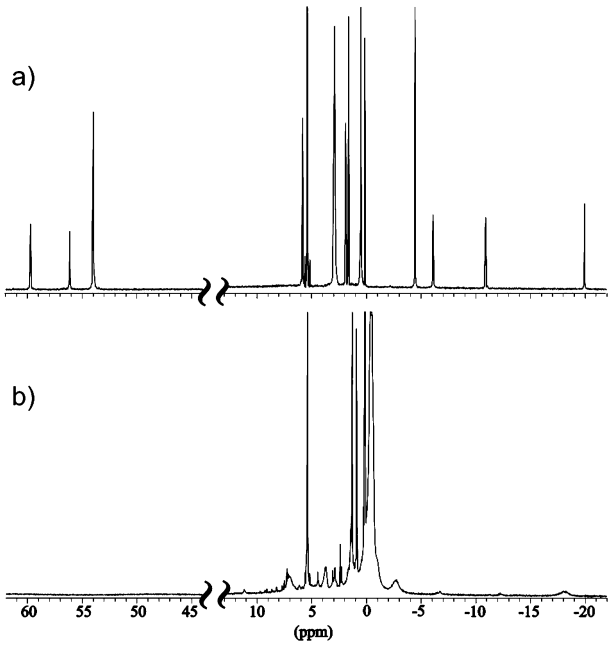

Figure 2. ^{1}H NMR spectra (400.13 MHz, 23 °C, CD_2Cl_2): (a) $CoCl_2N_2^{2ThE}$; (b) $CoCl_2N_2^{2ThE}$ after treatment with MAO (6 equiv).

6-phenyl derivative $CoCl_2N_2^{Ph}$,[1] as well as related dichloride Co^{II} complexes with 2,6-bis(imino)pyridine ligands,[17] the appearance of a signal typical for an $S = {}^1/_2$ effective spin Hamiltonian with largely anisotropic *g* values at low temperature can be attributed to large zero-field splitting (ZFS) effects of the $S = {}^3/_2$ state.[16,18]

In conclusion, the magnetic and spectroscopic characterization of the thien-3-yl complexes $CoCl_2N_2^{3Th}$ and $CoCl_2N_2^{3BT}$ and of the 6-bromo derivative $CoCl_2N_2^{Br}$ is strongly indicative of high-spin tetrahedral Co^{II} complexes both in the solid state and in solution.

The introduction of a pyridyl group in the 6-position of the pyridine ring of the (pyridin-2-yl)ethylidene-2,6-diisopropylbenzenamine moiety to give the ligand N_2^{Py} was achieved by the procedure illustrated in Scheme 3, while the picolyl-substituted ligand N_2^{PyMe} was obtained by the slightly different route illustrated in Scheme 4. The corresponding Co^{II} complexes $CoCl_2N_2^{Py}$ and $CoCl_2N_2^{PyMe}$ were synthesized as previously described for the related 6-(thienyl)-2-(imino)pyridine complexes and isolated as paramagnetic pale green crystals with a μ_{eff} value of about 4.8 μ_B at room temperature. However, unlike the 6-(organyl)-2-(imino)pyridine Co^{II} complexes, the metal center in $CoCl_2N_2^{Py}$ and $CoCl_2N_2^{PyMe}$ is five-coordinate, which is consistent with the stronger σ-ligating character of the pyridyl group vs that of the thienyl or phenyl groups in the other ligands. Convincing evidence for a five-coordinate complex was provided by the electronic spectra in both solution and the solid state, consisting of a pattern of bands with energy and relative intensity easily distinguishable from those of the tetrahedral Co^{II} complexes previously described.[1,2,19] As an example of the reliability of electron spectroscopy for distinguishing tetrahedral and five-coordinate Co^{II} complexes, Figure 1 shows the diffuse reflectance spectra of $CoCl_2N_2^{Ph}$ (a) and $CoCl_2N_2^{Py}$ (b). Noticeably, the spectral parameters of the latter complex are strongly indicative of a square-pyramidal geometry. Indeed, its absorption and reflectance spectra consist of five well-defined bands at 595, 650, 919, 1220, and 1790 nm and can be correlated with those of 2,6-bis(imino)pyridine Co^{II} dihalides.[17,20]

Like related dichloride Co^{II} complexes with 2,6-bis(imino)-pyridine ligands,[17] $CoCl_2N_2^{Py}$ and $CoCl_2N_2^{PyMe}$ did not show any EPR bands at room temperature, whereas a signal attributable to a broad and poorly resolved rhombic structure was observed below 10 K in CH_2Cl_2 frozen solution ($g_1 = 5.04(8)$, $g_2 = 3.00(8)$, and $g_3 = 1.95(8)$ for $CoCl_2N_2^{Py}$; $g_1 = 5.03(8)$, $g_2 = 3.00(8)$, and $g_3 = 1.94(8)$ for $CoCl_2N_2^{PyMe}$). The temperature dependence of each spectrum was consistent with the presence of large ZFS effects and fast spin−lattice relaxation times.[16,18]

Oligomerization of Ethylene Catalyzed by (Imino)pyridine Co^{II} Dichloride Complexes Activated by MAO. On activation by MAO in toluene, the complexes $CoCl_2N_2^{3Th}$ and $CoCl_2N_2^{3BT}$ were active catalysts for the selective dimerization of ethylene to 1-butene. Since the presence of residual $AlMe_3$ in commercial toluene solutions of MAO may lead to undesired reaction paths,[21,22] batch oligomerization and model activation reactions were carried out using solid MAO, obtained by careful removal

(17) Bianchini, C.; Mantovani, G.; Meli, A.; Migliacci, F.; Zanobini, F.; Laschi, F.; Sommazzi, A. *Eur. J. Inorg. Chem.* **2003**, 1620.

(18) (a) Drago, R. S. *Physical Methods for Chemists*; Saunders College: New York, 1992. (b) Mabbs, F. E.; Collison, D. *Electron Paramagnetic Resonance of d Transition Metal Complexes;* Elsevier: Amsterdam, 1992; Vol. 16. (c) Abragam, A.; Bleaney, B. *Electron Paramagnetic Resonance of Transition Ions*; Dover: New York, 1970. (d) Wertz, J. E.; Bolton, J. R. *Electron Spin Resonance: Elementary Theory and Practical Applications*; McGraw-Hill: New York, 1972. (e) Carlin, R. L. *Magnetochemistry*; Springer-Verlag: Berlin, 1986.

(19) (a) Cotton, F. A.; Wilkinson, G.; Murillo, C. A.; Bochmann, M. *Advanced Inorganic Chemistry*, 6th ed.; Wiley: New York, 1999; pp 814−835. (b) Morassi, R.; Sacconi, L. *J. Chem. Soc. A* **1971**, 492.

(20) (a) Sacconi, L.; Morassi, R.; Midollini, S. *J. Chem. Soc. A* **1968**, 1510. (b) Sacconi, L.; Bertini, I.; Morassi, R. *Inorg. Chem.* **1967**, *6*, 1548. (c) Ciampolini, M.; Speroni, G. P. *Inorg. Chem.* **1966**, *5*, 45.

(21) (a) Chen, E. Y.-X.; Marks, T. J. *Chem. Rev.* **2000**, *100*, 1391. (b) Busico, V.; Cipullo, R.; Cutillo, F.; Friederichs, N.; Ronca, S.; Wang, B. *J. Am. Chem. Soc.* **2003**, *125*, 12402.

(22) (a) Byun, D.-J.; Kim, S. Y. *Macromolecules* **2000**, *33*, 1921. (b) Britovsek, G. J. P.; Cohen, S. A.; Gibson, V. C.; Maddox, P. J.; van Meurs, M. *Angew. Chem., Int. Ed.* **2002**, *41*, 489. (c) Britovsek, G. J. P.; Bruce, M.; Gibson, V. C.; Kimberley, B. S.; Maddox, P. J.; Mastroianni, S.; McTavish, S. J.; Redshaw, C.; Solan, G. A.; Stromberg, S.; White, A. J. P.; Williams, D. J. *J. Am. Chem. Soc.* **1999**, *121*, 8728. (d) Semikolenova, N. V.; Zakharov, V. A.; Talsi, E. P.; Babushkin, D. E.; Sobolev, A. P.; Echevskaya, L. G.; Khysniayarov, M. M. *J. Mol. Catal. A: Chem.* **2002**, *182−183*, 283.

Table 2. ^{1}H NMR Parameters for $CoCl_2N_2^{2ThE}$ (400.13 MHz, 23 °C, CD_2Cl_2)

nucleus	δ (ppm)[a]
3-/5-Py	s, 59.71, 1H; s, 56.16, 1H
4-Py	s, −10.96, 1H
N=CCH$_3$	s, 54.00, 3H
3-/4-thiophene	s, −6.15, 1H; s, 1.28, 1H
m-Ph	d, 5.79, J = 5.0 Hz, 2H
p-Ph	t, −20.02, J = 5.0 Hz, 1H
CH_3^{iPr}	s, 2.86, 6H; s, 0.46, 6H
CH^{iPr}	s, 1.59, 2H
CH_2^{Et}	q, 1.85, J = 6.6 Hz, 2H
CH_3^{Et}	t, −4.49, J = 6.6 Hz, 3H

[a] Key: s, singlet; d, doublet; t, triplet; q, quartet.

Table 3. EPR Parameters Obtained from the Dichloride Catalyst Precursors with MAO (30 Equiv) in Toluene[a,b]

starting complex	g_x	g_y	g_z	a_x	a_y	a_z	g_{iso}	a_{iso}
$CoCl_2N_2Ph$	2.419	2.077	2.001	61	18	36	2.15	38
$CoCl_2N_2^{3Th}$	2.420	2.220	1.990	168	19	153	2.20	113
$CoCl_2N_2^{2ThE}$	2.195	2.030	2.024	107	166	43	2.07	105
$CoCl_2N_2^{Py}$	2.290	2.025	2.017	84	19	47	2.11	50
$CoCl_2N_2^{PyMe}$	2.290	2.029	2.015	81	20	50	2.12	52

[a] The g_{iso} values were obtained from room-temperature spectra. [b] The g_i and a_i (expressed in gauss) values were obtained by simulation of the frozen-solution spectra. The a_{iso} values were calculated as the average of the three hyperfine coupling constants.

of solvent and volatile impurities from commercial MAO under reduced pressure.[22d]

The addition of ethylene to the catalyst/cocatalyst mixture resulted in a rapid exotherm, indicative of no induction period. Selected data are reported in Table 1, which also contains data obtained with the precursors $CoCl_2N_2^{2Th}$, $CoCl_2N_2^{2BT}$, $CoCl_2N_2^{2ThE}$, and $CoCl_2N_2^{Ph}$ under comparable experimental conditions.

At 5 bar of C_2H_4, both the TOF (ca. 1×10^5 mol of C_2H_4 converted (mol of Co)$^{-1}$ h^{-1}) and the selectivity shown by $CoCl_2N_2^{3Th}$ and $CoCl_2N_2^{3BT}$ were comparable to those of $CoCl_2N_2^{Ph}$ (entries 2, 5, and 6). In contrast, the thien-2-yl regioisomers $CoCl_2N_2^{2Th}$, $CoCl_2N_2^{2ThE}$ and $CoCl_2N_2^{2BT}$, were 5−10 times more active and gave low-molecular-weight α-olefins (C_4−C_{14}) with Schulz−Flory distributions and more than 90% selectivity (entries 1, 3, and 4; Table 1). The internal olefins showed predominantly *E* conformations (>70%), while no branched product was observed. Consistent with the use of solid MAO, neither saturated hydrocarbons nor odd olefins, due to chain transfer to aluminum, were produced.[22] The significant isomerization to internal alkenes indicates β-H transfer to metal as an effective chain transfer mechanism.[1,2,4] For all catalysts, the TOF is linear with the C_2H_4 pressure, which suggests that the major catalyst resting state is a cobalt alkyl complex.[1,2,4]

Under the experimental conditions reported in Table 1, no ethylene oligomerization activity at all was observed using $CoCl_2N_2^{Br}$, $CoCl_2N_2^{Py}$, or $CoCl_2N_2^{PyMe}$ as catalyst precursor.

Activation of the Dichloride Catalyst Precursors by MAO. Product analysis and studies on the dependence of the activity and Schulz−Flory α values on ethylene pressure have been useful tools to elucidate the propagation and chain transfer mechanisms of ethylene oligomerization by the (imino)pyridine Co^{II} catalysts previously studied.[1,2] It was established that propagation occurs via a Cossee−Arlman mechanism and chain transfer proceeds by β-H transfer to metal, although the concomitant occurrence of β-H transfer to monomer cannot be ruled out.[4c] Unfortunately, the large excess of MAO required to have high oligomerization activity makes in situ spectroscopic studies, such as NMR and IR, unable to provide detailed information on the initiation step. Moreover, catalytically relevant species might not be sufficiently long-lived to be intercepted on the IR and NMR time scale, while tetrahedral Co^{II} complexes are not particularly amenable to be studied by NMR spectroscopy due to their paramagnetic nature. Nevertheless, as shown by the ^{1}H NMR spectra acquired in CD_2Cl_2 solution for $CoCl_2N_2^{2ThE}$ before (a) and after treatment with MAO (6 equiv) (b), some useful information may be obtained on the MAO-activated product (Figure 2).

Scheme 5

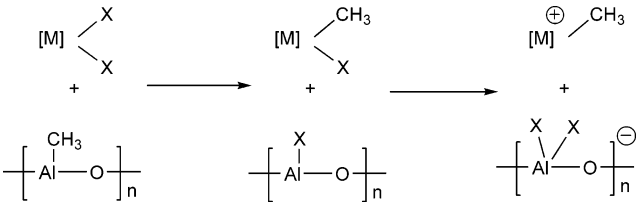

In the absence of MAO, all protons resonate at chemical shifts significantly different from those of the corresponding protons in the free ligand N_2^{2ThE}, which is consistent with the presence of three unpaired electrons in the cobalt complex. Unambiguous signal assignment was achieved on the basis of isotropic shifts essentially attributable to a Fermi contact contribution (Table 2).[23]

In line with the coordination of cobalt through the two nitrogen atoms, the largest paramagnetic shifts were exhibited by the nuclei in the 3- and 5-positions of the pyridine ring (δ 56.16 and 59.71) and by the protons of the CH$_3$C=N group (δ 54.00). The addition of 6 equiv of MAO in 2 equiv portions dramatically changed the spectrum. A remarkable line broadening of the original resonances occurred just after adding the first 2 equiv of activator. Concomitantly, new, relatively sharp resonances appeared in the 2−10 ppm region, which were not present in the ^{1}H NMR spectrum of MAO alone. After the third portion of MAO was added, no clear signal was observed in the region downfield to 12 ppm, while new signals appeared at negative chemical shift values.

Overall, this picture suggests that the addition of MAO does not convert the parent complex into a diamagnetic species, as occurs for 2,6-bis(imino)pyridine Co^{II} dihalides.[24] Indeed, as shown also by the following EPR study, as well as in situ magnetic moment measurements, the activated product maintains paramagnetic features, although a decrease in the magnetic moment may be envisaged in view of the higher concentration of signals in the region of diamagnetic molecules.

In Situ EPR Study. The inability of NMR spectroscopy to provide further information on the MAO-activated species prompted us to carry out an EPR study. In fact, EPR spectroscopy is much more amenable than NMR spectroscopy to intercept and characterize elusive paramagnetic species.

As previously said, tetrahedral (imino)pyridine Co^{II} complexes are EPR-silent at room temperature. It was therefore interesting to find out that $CoCl_2N_2^{Ph}$, $CoCl_2N_2^{2ThE}$, $CoCl_2N_2^{3Th}$, $CoCl_2N_2^{Py}$, and $CoCl_2N_2^{PyMe}$ were transformed into products already showing EPR signals at room temperature on treatment with 30 equiv of MAO in toluene. In all cases, the spectra did not show any hyperfine structure and were unequivocally

(23) (a) Jesson, J. P. *NMR of Paramagnetic Molecules: Principles and Applications*; La Mar, G. N., Horrocks, W. D., Holm, R. H., Eds.; Academic Press: New York, 1973. (b) Holm, R. H.; Phillips, W. D.; Averill, B. A.; Mayerle, J. J.; Herskovitz, T. *J. Am. Chem. Soc.* **1974**, *96*, 2109. (c) McConnell, H. M. *Proc. Natl. Acad. Sci. U.S.A.* **1972**, *69*, 335.

(24) Humphries, M. J.; Tellmann, K. P.; Gibson, V. C.; White, A. J. P.; Williams, D. J. *Organometallics* **2005**, *24*, 2039.

Chart 1

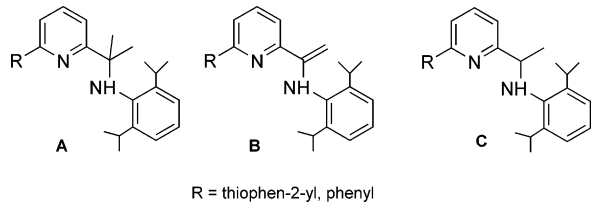

attributed to low-spin Co^{II} species ($S = {}^1/_2$) with the expected g_{iso} values (Table 3). Identical signals were seen when the EPR spectra were acquired in the presence of ethylene: i.e., under truly operando conditions.

The magnetic moments of the species generated by treatment of the high-spin precursors with MAO were estimated by means of the Evans method[25] using cyclohexane as the inert probe substance.[25e] Values of the magnetic moments in the range of 1.8−2.3 μ_B were calculated, which confirms the quantitative transformation of the high-spin Co^{II} precursors into low-spin Co^{II} products.[26−28]

Before making any comment on and interpretation of the EPR spectra, it is worthwhile to recall the general mechanism by which MAO can activate early- and late-metal halide complexes for alkene insertion. As shown in Scheme 5, a well-established function of MAO is to replace halide ligands with methyl groups and ultimately create a ion pair made of a coordinatively unsaturated complex cation and $[MAO]^-$ anions.[21]

Other relevant roles of MAO, such as reducing agent, hydrogen abstractor, C-alkylating agent and O-ligand, have been also reported,[21,22,24] yet no evidence of their occurrence in the present reactions was obtained. In particular, several experiments have been performed which clearly show that the (imino)-pyridine ligands are not modified by the activator under catalytic conditions. The complexes $CoCl_2N_2^{2Th}$ and $CoCl_2N_2^{Ph}$ were suspended in toluene and then treated with an excess of MAO (30−200 equiv). After they were stirred for 1−30 min at room temperature, the resulting reaction mixtures were quenched with MeOH/HCl. The extracted organic residue was shown by NMR spectroscopy to be the intact (imino)pyridine ligand. Other possible modifications of the (imino)pyridine ligands, such as C-alkylation (**A**),[29] H-abstraction[30] (**B**), and hydride addition (**C**), were not observed (Chart 1).

Scheme 6

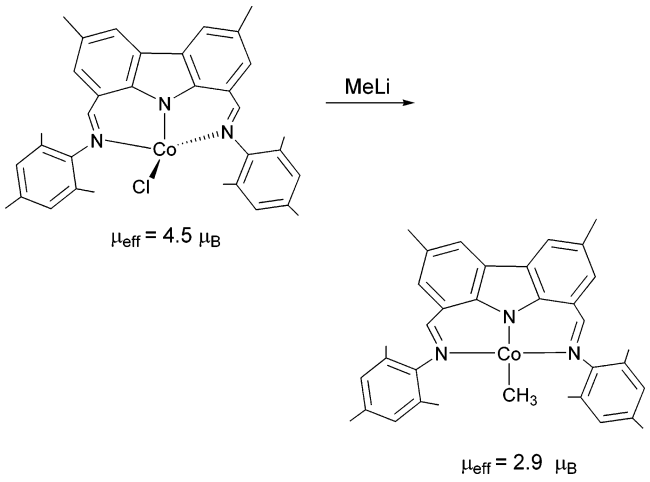

In order to obtain these products, the ligands must be treated with the appropriate reagents under specific experimental conditions: $AlMe_3$ in refluxing toluene,[31] product **A**; MeLi in THF at −50 °C, product **B**; $LiAlH_4$ in refluxing THF, product **C**.[32,33]

Having established that the activation of the cobalt precursors with MAO does not affect the structure of the supporting (imino)pyridine ligand, we need to explain the EPR results. The simple substitution of the chlorides in the precursors with stronger methyl ligands by MAO cannot account for the appearance of an EPR signal at room temperature without a concomitant change in the coordination geometry from high-spin tetrahedral to low-spin square planar or five-coordinate.

Five-coordination is much more unlikely than four-coordination, as the number of available donor atoms in the precursors and, to a major extent, in the activated species is limited to a maximum of three or four. Moreover, although not numerous, some examples of low-spin square-planar Co^{II} complexes with nitrogen ligands are known,[26−28] among which it is worth highlighting a 1,8-bis(imino)carbazolide complex obtained by replacing chloride with methyl in a tetrahedral precursor (Scheme 6).[28] Other four-coordinate geometries, such as the pseudotetrahedral geometry exhibited by the doublet ground state Co^{II} complex $CoI[PhBP_3]$ ($PhBP_3 = PhB(CH_2PPh_2)_3^-$), can be considered unlikely, as they are strongly related to the tripodal geometry of the supporting ligand.[34]

In conclusion, the formation of square-planar Co^{II} species upon activation with MAO of the tetrahedral precursors $CoCl_2N_2^{Ph}$, $CoCl_2N_2^{2ThE}$, and $CoCl_2N_2^{3Th}$ was immediately considered as highly probable.

In an attempt to obtain structural information, a variable-temperature EPR study was conducted on the MAO-activated products. Frozen spectra at 5 K are reported in Figure 3 as solid lines.

The spectra, typical for low-spin Co^{II} species ($S = {}^1/_2$, $I = {}^7/_2$), show large and resolved g and a anisotropy and are characterized by a complex structure due to the superposition of the different components of the anisotropic hyperfine

(25) (a) Evans, D. F. *J. Chem. Soc.* **1959**, 2003. (b) Evans, D. F.; Fazakerley, G. V.; Phillips, P. R. F. *J. Chem. Soc. A* **1971**, 1931. (c) Crawford, H. D.; Swanson, J. *J. Chem. Educ.* **1971**, *48*, 382. (d) Grant, D. H. *J. Chem. Educ.* **1995**, *72*, 39. (e) Britovsek, G. J. P.; Gibson, V. C.; Spitzmesser, S. K.; Tellmann, K. P.; White, A. J. P.; Williams, D. J. *Dalton Trans*. **2002**, 1159.

(26) Bodreaux, E. A.; Mulay, L. N. *Theory and Applications of Molecular Paramagnetism*; Wiley: New York, 1976; pp 211−225.

(27) (a) Muller, G.; Sales, J.; Torra, I.; Vinaixa, J. *J. Organomet. Chem.* **1982**, *224*, 189. (b) Anton, M.; Muller, G.; Sales, J.; Vinaixa, J. *J. Organomet. Chem.* **1982**, *239*, 365. (c) Beattie, J. K.; Hambley, T. W.; Klepetko, J. A.; Masters, A. F.; Turner, P. *Polyhedron* **1996**, *15*, 473. (d) Jaynes, B. S.; Doerrer, L. H.; Liu, S.; Lippard, S. J. *Inorg. Chem.* **1995**, *34*, 5735. (e) Fryzuk, M. D.; Leznoff, D. B.; Thompson, R. C.; Retting, S. J. *J. Am. Chem. Soc.*, **1998**, *120*, 10126.

(28) Gibson, V. C.; Spitzmesser, S. K.; White, A. J. P.; Williams, D. J. *Dalton Trans*. **2003**, 2718.

(29) (a) Bruce, M.; Gibson, V. C.; Redshaw, C.; Solan, G. A.; White, A. J. P.; Williams, D. J. *Chem. Commun.* **1998**, 2523. (b) Milione, S.; Cavallo, G.; Tedesco, C.; Grassi, A. *Dalton Trans.* **2002**, 1839. (c) Knijnenburg, Q.; Smits, J. M. M.; Budzelaar, P. H. M. *Organometallics* **2006**, *25*, 1036.

(30) (a) Khorobkov, I.; Gambarotta, S.; Yap, G. P. A.; Budzelaar, P. H. M. *Organometallics* **2002**, *21*, 3088. (b) Sugiyama, H.; Gambarotta, S.; Yap, G. P. A.; Wilson, D. R.; Thiele, S. K.-H. *Organometallics* **2004**, *23*, 5054. (c) Blackmore, I. J.; Gibson, V. C.; Hitchcock, P. B.; Rees, C. W.; Williams, D. J.; White, A. J. P. *J. Am. Chem. Soc.* **2005**, *127*, 6012. (d) Bouwkamp, M. W.; Lobkovsky, E.; Chirik, P. J. *Inorg. Chem.* **2006**, *45*, 2.

(31) Gibson, C. V.; Redshaw, C.; White, A. J. P.; Williams, D. J. *J. Organomet. Chem.* **1998**, *550*, 453.

(32) Bianchini, C.; Giambastiani, G. Unpublished results.

(33) For MAOs which can contain and/or are able to generate aluminum hydride species see: (a) Rogers, J. S.; Bazan, G. C. *Chem. Commun.* **2000**, 1209. (b) Hagen, H.; Kretschmer, W. P.; van Buren, F. R.; Hessen, B.; van Oeffelen, D. A. *J. Mol. Catal. A: Chem.* **2006**, *248*, 237.

(34) Jenkins, D. M.; Di Bilio, A. J.; Allen, M. J.; Betley, T. A.; Peters, J. C. *J. Am. Chem. Soc.* **2002**, *124*, 15336.

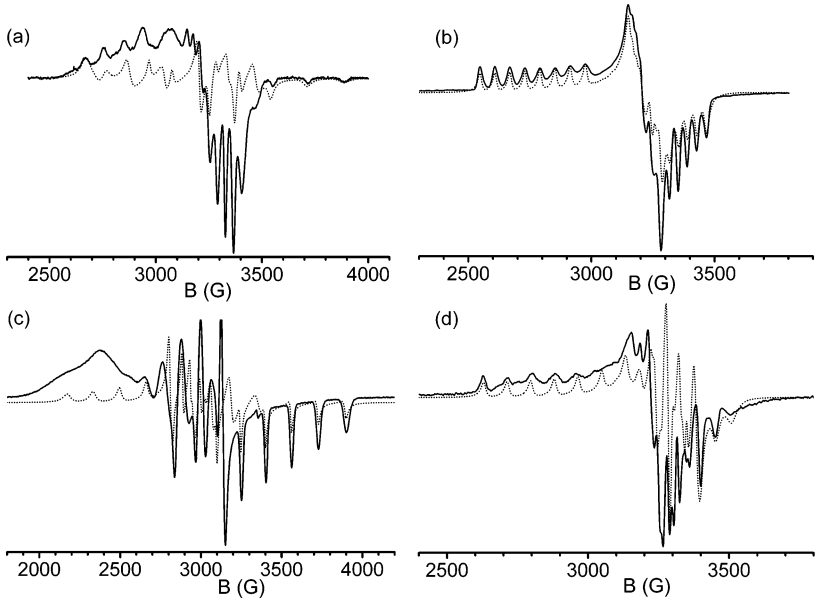

Figure 3. Frozen CH_2Cl_2 solution (5 K) X-band EPR spectra of MAO-activated (a) $CoCl_2N_2^{2ThE}$, (b) $CoCl_2N_2^{Ph}$, (c) $CoCl_2N_2^{3Th}$, and (d) $CoCl_2N_2^{Py}$ together with best simulations (dotted lines) obtained with parameters reported in Table 3.

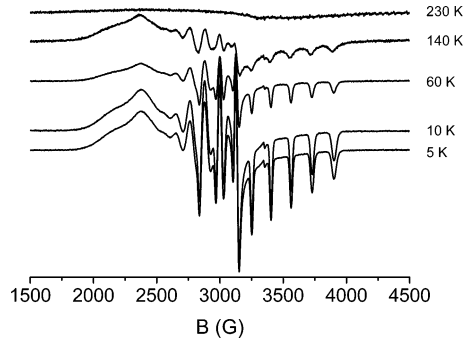

Figure 4. Temperature variation of X-band EPR spectrum of $CoCl_2N_2^{3Th}$/MAO (30 equiv).

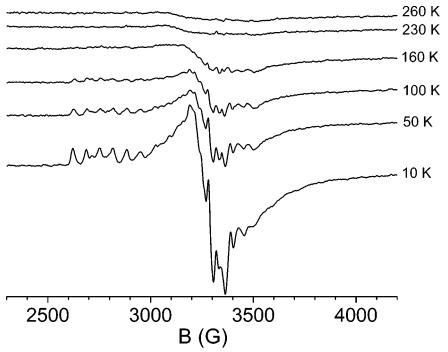

Figure 5. Temperature variation of X-band EPR spectrum of $CoCl_2N_2^{PyMe}$/MAO (30 equiv).

coupling. Due to the broadness of the hyperfine lines, no superhyperfine structure was observed, notwithstanding the likely delocalization of some unpaired spin density on nitrogen and/or hydrogen atoms of the (imino)pyridine ligand, as indicated by theoretical calculations (vide infra). Each spectrum was simulated to get the corresponding anisotropic parameters (Table 3), and the results of the simulations are shown in Figure 3 as dotted lines. To reduce the number of parameters for the simulation process, no quadrupolar term was introduced in the spin Hamiltonian used for the simulation: $H = \beta \mathbf{B}\cdot\mathbf{g}\cdot\mathbf{S} + \mathbf{S}\cdot\mathbf{A}\cdot\mathbf{I}$.[35] In view of the spin Hamiltonian parameters for best simulated curves, it is apparent that $CoCl_2N_2^{2ThE}$ is characterized by a nearly axial spectrum, while the spectra of $CoCl_2N_2^{Ph}$ and $CoCl_2N_2^{3Th}$ are rhombic.

Different factors may account for the observed discrepancies between the experimental and simulated spectra of $CoCl_2N_2^{2ThE}$ (central part of the spectrum, Figure 3a) and $CoCl_2N_2^{3Th}$ (low-field part of the spectrum, Figure 3c). An important factor might be the presence of a second species, likely a residual amount of the starting complex, whose spectrum superimposes onto the spectrum of the MAO-activated species. Anomalous line-broadening effects, connected with low-lying excited states, or our choice to neglect the quadrupolar term may also have contributed to the nonperfect agreement of the experimental and computed spectra of $CoCl_2N_2^{2ThE}$ and $CoCl_2N_2^{3Th}$. Finally, the simulation of low-spin Co^{II} spectra might be made difficult by the fact that the *g* and *a* principal directions may be non-collinear, an effect that has been neglected in the present approach.[18b,36] On the other hand, for all compounds, the experimental g_{iso} values were in good agreement with the values obtained from the average of the three principal g_i values ($i = x, y, z$) of the frozen-solution spectra, which is an indirect confirmation of the overall validity of the simulations.

It is worth noticing that the product generated by $CoCl_2N_2^{Ph}$ shows a frozen EPR spectrum with hyperfine interactions smaller than those of the products obtained from $CoCl_2N_2^{2ThE}$ and $CoCl_2N_2^{3Th}$. The relation between the *a* values and the electronic configuration of Co^{II} metal ions is very subtle, as it may depend on as many as 12 parameters.[16,36,37] In the absence of an in-depth study, which is out of the scope of this article, the only comment we can make is that the energies of the excited quartet states, which, in a perturbative approach, contribute to the third order in *g* values and to the second order in *a* values, are substantially different in $CoCl_2N_2^{Ph}$ as compared to $CoCl_2N_2^{2ThE}$ and $CoCl_2N_2^{3Th}$.

All of the EPR spectra of the MAO-activated complexes showed identical behavior with temperature. As an example,

(35) Jacobsen, C. J. H.; Pedersen, E.; Villadsen, J.; Weihe, H. *Inorg. Chem.* **1993**, *32*, 1216.

(36) Daul, C.; Schlapfer, C. W.; von Zelewsky, A. In *Structure and Bonding*; Dunitz, J. D., Ed.; Springer-Verlag: Berlin, 1979; Vol. 36, p 129.

(37) McGarvey, B. R. *Can. J. Chem.* **1975**, *53*, 2498.

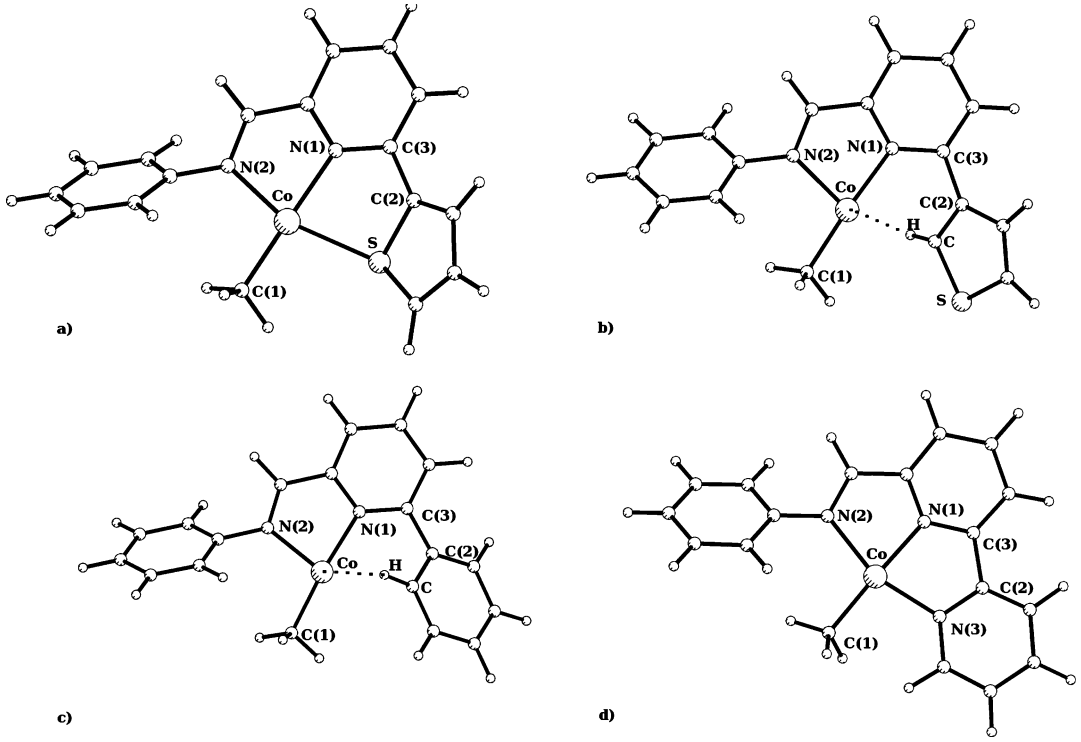

Figure 6. Optimized models of (a) $[Co(CH_3)N_2{}^{2Th}]^+$, (b) $[Co(CH_3)N_2{}^{3Th}]^+$, (c) $[Co(CH_3)N_2{}^{Ph}]^+$, and (d) $[Co(CH_3)N_2{}^{Py}]^+$.

Table 4. Selected Bond Lengths (Å) and Angles (deg) for the Four Models

	$[Co(CH_3)N_2{}^{2Th}]^+$	$[Co(CH_3)N_2{}^{3Th}]^+$	$[Co(CH_3)N_2{}^{Py}]^+$	$[Co(CH_3)N_2{}^{Ph}]^+$
Co−X[a]	2.40	2.53	2.04	2.71
Co−N(1)	2.03	1.99	1.95	2.01
Co−N(2)	2.00	2.01	2.04	1.98
Co−C(1)	1.94	1.93	1.94	1.92
Co−H		2.36		2.33
N(1)−Co−C(1)	179	177	175	176
N(2)−Co−X	159	153	160	149
X[a]−C(2)−C(3)−N(1)	20	37	1.7	22

[a] X is the sulfur atom for $[Co(CH_3)N_2{}^{2Th}]^+$, the agostic carbon atom for $[Co(CH_3)N_2{}^{3Th}]^+$ and $[Co(CH_3)N_2{}^{Ph}]^+$, and the N(3) nitrogen atom for $[Co(CH_3)N_2{}^{Py}]^+$.

Scheme 7

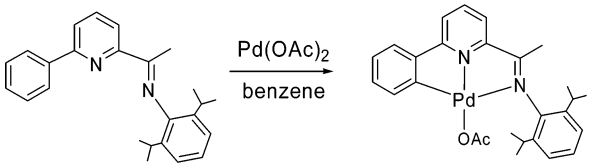

the spectra of $CoCl_2N_2{}^{3Th}$ taken in the temperature interval from 5 and 230 K are reported in Figure 4.

Increasing the temperature from 5 to 160 K caused line broadening as well as a decrease of the spectral intensity; however, no evidence whatsoever of a spin-state transition to a high-spin configuration was observed. The major variation was noticed above 180 K, where the solutions became fluid and the spectrum lost any hyperfine structure due to a large line broadening, which suggests the anisotropic hyperfine interactions were not completely mediated.[16b]

A clear EPR signal was seen already at room temperature by reacting the five-coordinate complex $CoCl_2N_2{}^{PyMe}$ in toluene with MAO. A sequence of variable-temperature EPR spectra of the system $CoCl_2N_2{}^{PyMe}$/MAO are reported in Figure 5.

Scheme 8

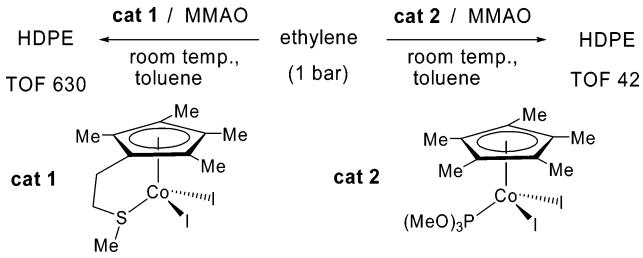

The spectral parameters of the spectrum for this species at 10 K as well as its temperature dependence are in line with those observed for all the other MAO-activated Co^{II} precursors (Table 3) and are attributable to a low-spin square-planar Co^{II}−methyl complex.

It is noteworthy that the two MAO-activated complexes that do not contain a potentially coordinating heteroatom (i.e., $[Co(CH_3)N_2{}^{Ph}]^+$ and $[Co(CH_3)N_2{}^{3Th}]^+$) have similar g_x values (∼2.42), while the compounds eventually stabilized by a σ-bond with sulfur or nitrogen (i.e., $[Co(CH_3)N_2{}^{2Th}]^+$, $[Co(CH_3)N_2{}^{Py}]^+$, and $[Co(CH_3)N_2{}^{PyMe}]^+$) exhibit much smaller g_x values (2.2−2.3).

In conclusion, the EPR study has unambiguously demonstrated the occurrence of a spin state changeover in the activation of the catalyst precursors by MAO. The most likely coordination geometry of the Co^{II} centers in the activated species is square planar with two nitrogen atoms from the (imino)pyridine ligand, a carbon atom from a methyl group released by MAO, and a fourth ligand that *might be provided by the organyl group in the 6-position of the pyridine ring*. Indeed, in the absence of either ring, as in $CoCl_2N_2{}^{Br}$, no EPR signal appeared on treatment of the complex in toluene with an excess of MAO in the temperature range from 293 to 20 K. It is therefore very likely that the organyl group in the 6-position interacts with the cobalt center.

Chart 2

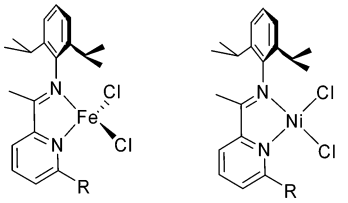

R = Ph, thiophen-2-yl

DFT Modeling Study of the MAO-Activated Species. In an attempt to elucidate the structure of the low-spin Co^{II} species, we built up four models of the low-spin complex cations $[Co(CH_3)N_2^{2Th}]^+$, $[Co(CH_3)N_2^{Ph}]^+$, $[Co(CH_3)N_2^{3Th}]^+$, and $[Co(CH_3)N_2^{Py}]^+$ generated by the reaction of MAO with the corresponding dichloride precursors. The optimized structures are reported in Figure 6, while selected bond distances and angles are given in Table 4. Models for high-spin species were not considered, in light of the experimental EPR and NMR (Evans method) evidence for the exclusive formation of low-spin species.

In all optimized structures, the cobalt atom turned out to be at the center of a distorted square plane with three coordination positions occupied by the N_2C donor atom set. Neither the geometry nor the stereochemistry of this portion of the complex cations changes in the three models. In contrast, the four models differ in the atom occupying the fourth position of the square plane. This position is occupied by the thien-2-yl sulfur atom in $[Co(CH_3)N_2^{2Th}]^+$ or by a nitrogen atom in $[Co(CH_3)N_2^{Py}]^+$, whereas an agostic C−H group would complete the square-planar coordination in $[Co(CH_3)N_2^{Ph}]^+$ and $[Co(CH_3)N_2^{3Th}]^+$. The $Co-H_{agostic}$ distance is quite the same in the latter complexes, whereas, due to the different internal angles of the thien-3-yl and phenyl rings, the $Co-C_{agostic}$ distance in $[Co(CH_3)N_2^{Ph}]^+$ is almost 0.2 Å longer than in $[Co(CH_3)N_2^{3Th}]^+$. The complex $[Co(CH_3)N_2^{2Th}]^+$ is appreciably more stable (around 6 kcal/mol) than the regioisomer $[Co(CH_3)N_2^{3Th}]^+$. The interaction between the metal and the atom in the fourth position of the square plane was estimated by allowing the organyl groups in the pyridine 6-position to rotate about the C(2)−C(3) bond. For $[Co(CH_3)N_2^{2Th}]^+$ and $[Co(CH_3)N_2^{Py}]^+$ the maximum energy was found for the organyl group perpendicular to the (imino)pyridine plane and the energy gap between this conformer and the optimized structure was around 15 and 38 kcal/mol, respectively. The same conformers of $[Co(CH_3)N_2^{Ph}]^+$ and $[Co(CH_3)N_2^{3Th}]^+$ were destabilized with respect to the optimized geometry by 6 and 9 kcal/mol, respectively. Notably, the energy barriers to the rotation of the thien-3-yl and phenyl rings around the C(2)−C(3) bond are the same in the free ligands (5.5 kcal/mol), which confirms that it is the interaction with the metal that makes the complexes different from each other.

It is worth mentioning that ortho metalation, the potential fate of any C−H−metal agostic interaction, is a feasible reaction opportunity for the ligand N_2^{Ph}, provided there is a suitable metal fragment (Scheme 7).[38]

For all complexes, the calculated total spin density is mainly located on cobalt (the value of the spin density for the cobalt atom is between 1.17 for $[Co(CH_3)N_2^{Ph}]^+$ and 1.23 for $[Co(CH_3)N_2^{Py}]^+$; see the Supporting Information), while the methyl bonded to the metal has a negative spin density of about 0.2.

Scheme 9

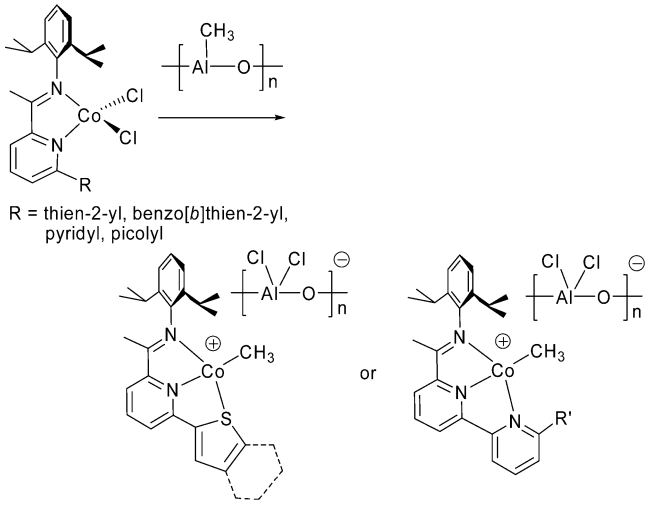

Discussion

The presence of an aromatic group bearing a weakly coordinating donor atom (e.g., a thienyl sulfur such as in $CoCl_2N_2^{2Th}$ and $CoCl_2N_2^{2BT}$) in the 6-position of the pyridine ring of the supporting ligand and the low-spin d^7 configuration of the MAO-activated cobalt center seem to be key factors for promoting the oligomerization activity of the present (imino)-pyridine dichloride Co^{II} precursors.[6] The importance of ligand hemilability in assisting insertion polymerization by cobalt catalysis has been previously demonstrated by Brookhart.[40] This author showed that the substitution of a tertiary phosphine/phosphite with a hemilabile thioether ligand increases remarkably the ability of cyclopentadienyl Co^{III} complexes to catalyze the polymerization of ethylene to high-density polyethylene (HDPE) (Scheme 8). It was suggested that the sulfur atom lowers the barrier to ethylene insertion through the stabilization of the electron-deficient transition state for migratory insertion.

No useful information was found in the relevant literature, which might account for the role exerted by the low-spin d^7 electronic configuration observed in the square-planar Co^{II} propagating alkyls. Nor we have a reliable explanation for it. On the other hand, neither the tetrahedral high-spin d^6 Fe^{II} complexes $FeCl_2N_2^{Ph}$ and $FeCl_2N_2^{2Th}$ nor the square-planar diamagnetic d^8 Ni^{II} complexes $NiCl_2N_2^{Ph}$ and $NiCl_2N_2^{2Th}$ (Chart 2) have been found to catalyze the oligomerization/polymerization of ethylene on treatment with MAO under the experimental conditions of Table 1.[3]

Incorporation of these data with the experimental and theoretical pieces of evidence suggests that the precursors $CoCl_2N_2^{2Th}$, $CoCl_2N_2^{2BT}$, $CoCl_2N_2^{Py}$, and $CoCl_2N_2^{PyMe}$ are transformed by MAO in toluene into square-planar Co^{II} complexes where a coordination position is occupied by sulfur or nitrogen (Scheme 9).

Once the square-planar methyl complex cations are formed, they will have to bind a cis ethylene molecule to undergo methyl migratory insertion and produce α-olefins by successive ethylene trapping/migratory insertion cycles, followed eventually by β-H transfer termination. The lack of any activity of $CoCl_2N_2^{Py}$ and $CoCl_2N_2^{PyMe}$ may be therefore ascribed to the strong bonding interaction between cobalt and the nitrogen atom of the

(38) Bianchini, C.; Lenoble, G.; Oberhauser, W.; Parisel, S.; Zanobini, F. *Eur. J. Inorg. Chem.* **2005**, 4794

(39) Bianchini, C.; Giambastiani, G.; Guerrero Rios, I.; Mantovani, G.; Meli, A.; Segarra, A. M. *Coord. Chem. Rev.* **2006**, *250*, 1391.

(40) Daugulis, O.; Brookhart, M.; White, P. S. *Organometallics* **2003**, *22*, 4699.

Scheme 10

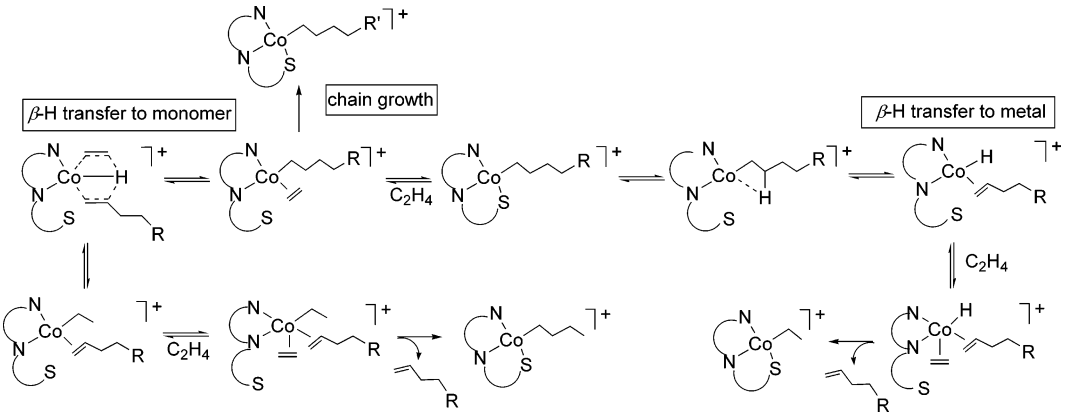

peripheral pyridine ring, which does not allow for monomer activation.

Apparently, the presence of a thien-2-yl sulfur in the propagating alkyl species is not an obstacle to monomer coordination, as both $CoCl_2N_2^{2Th}$ and $CoCl_2N_2^{2BT}$ are very active for ethylene oligomerization, yielding C_4-C_{14} α-olefins. In a sense, the role of the sulfur atom in the thien-2-yl Co^{II} precursors may be similar to that proposed for the sulfur in the thioether $CpCo^{III}$ complex shown in Scheme 8. Just the production of C_4-C_{14} α-olefins with a Schulz−Flory distribution indicates that the thien-2-yl sulfur competes with ethylene for coordination to cobalt, retarding chain transfer vs chain propagation. After only six to seven consecutive insertions does the chain transfer rate definitely prevail over the propagation rate, likely due to steric reasons. The square-planar structure of the propagating alkyl, its character of catalyst resting state, and the occurrence of olefin isomerization are strongly reminiscent of the catalytic mechanism of diamagnetic α-diimine Ni^{II} and Pd^{II} complexes in which the termination proceeds via associative displacement, irrespective of the chain transfer mechanism (β-H transfer to metal or monomer) (Scheme 10).[4c,41] In this picture, the role of the thien-2-yl sulfur atom would be that of disfavoring ethylene coordination, destabilizing the transition state to α-olefin elimination.

The energy barriers to rotation of the phenyl and thien-3-yl rings calculated for the square-planar methyl complexes $[Co(CH_3)N_2^{Ph}]^+$ and $[Co(CH_3)N_2^{3Th}]^+$, although in line with agostic interactions, are too low (6 and 9 kcal mol^{-1}, respectively) to be taken as unambiguous proof for propagating alkyls with the structure shown in Scheme 11. Indeed, under real catalytic conditions, ethylene, toluene, and even $[MAO]^-$ might compete with the agostic interaction.

It is a fact, however, that both $CoCl_2N_2^{Ph}$ and $CoCl_2N_2^{3Th}$ are as active as the thien-2-yl substituted catalysts but are selective for 1-butene production, which is consistent with a much faster β-H transfer from the butenyl group as compared to its migratory insertion into the monomer. Since the termination occurs by associative displacement of ethylene (the chain transfer rate is first order in ethylene concentration),[1,2] it is very likely that the phenyl and thien-3-yl groups in the 6-position are sterically and electronically appropriate to stabilize the transition state to α-olefin elimination just after the second monomer insertion.

(41) (a) Killian, C. M.; Johnson, L. K.; Brookhart, M. *J. Am. Chem. Soc.* **1995**, *117*, 6414. (b) Killian, C. M.; Johnson, L. K.; Brookhart, M. *Organometallics* **1997**, *16*, 2005. (c) Svejda, S. A.; Brookhart, M. *Organometallics* **1999**, *18*, 65.

Scheme 11

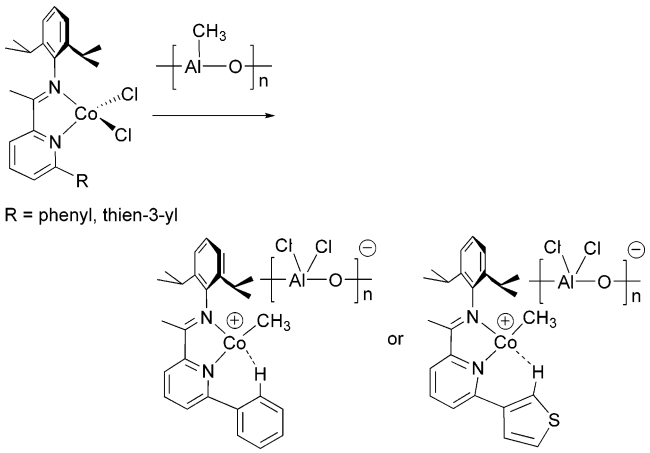

Conclusions

The position of the sulfur atom in the thienyl group of 6-(thienyl)-2-(imino)pyridine ligands has been found to control both the catalytic activity and selectivity of the corresponding tetrahedral dihalide Co^{II} complexes in the oligomerization of ethylene to α-olefins upon activation with MAO. Complexes with the sulfur atom in the 3-position of the thienyl ring catalyze the selective conversion of ethylene to 1-butene, while catalysts containing thien-2-yl groups give C_4-C_{14} α-olefins. Given the comparable sizes of the thiophen-3-yl and benzo[*b*]thiophen-3-yl groups as compared to thiophen-2-yl and benzo[*b*]thiophen-2-yl groups, steric factors cannot account for the remarkably different selectivity of the corresponding catalysts.

In situ EPR experiments have shown that all of the high-spin Co^{II} precursors undergo a spin state changeover with formation of low-spin Co^{II} propagating alkyls of the formula $[CoN_2(alkyl)]^+$. DFT calculations on the latter compounds are consistent with the coordination of the sulfur atom only for the thien-2-yl derivatives. The fastening/unfastening of the sulfur atom in the thien-2-yl complexes is suggested, on one hand, to stabilize the electron-deficient transition state for migratory insertion and, on the other hand, to retard chain transfer by destabilizing the transition state to α-olefin elimination. The results of the DFT study of the $[CoN_2(alkyl)]^+$ complexes bearing thien-3-yl and phenyl substituents are much less conclusive, as the stabilizing energy of possible C−H agostic species is too low (6−9 kcal/mol) to draw out a reliable mechanistic rationale for the observed selectivity. On the other hand, the presence of an aromatic group in the 6-position of the central pyridine ring is mandatory for ethylene oligomer-

ization, as (imino)pyridine ligands with no substituent in this position are catalytically inactive. Likewise, a strong donor atom in the 6-position, as in the 2-pyridyl substituted ligands, inhibits the catalytic activity.

Acknowledgment. Thanks are due to the European Community (STREP Project No. 516972-NANOHYBRID; Network of Excellence IDECAT) and the Ministero dell'Istruzione, dell'Università e della Ricerca (FIRB Project No. RBNE03R78E-NANOPACK) for financial support. The computations were carried out at the CINECA of Bologna under the agreement CINECA-CNR. L.S. and D.G. acknowledge the financial support of Ente Cassa Risparmio di Firenze and of Ministero dell'Istruzione, dell'Università e della Ricerca (PRIN 2005).

Supporting Information Available: Figures giving powder EPR spectra of $CoCl_2N_2^{Br}$, $CoCl_2N_2^{3Th}$, and $CoCl_2N_2^{2Th}$ at 10 K and tables giving Cartesian coordinates and α spin densities of the model cations $[Co(CH_3)N_2^{2Th}]^+$, $[Co(CH_3)N_2^{3Th}]^+$, $[Co(CH_3)N_2^{Py}]^+$, and $[Co(CH_3)N_2^{Ph}]^+$. This material is available free of charge via the Internet at http://pubs.acs.org.

OM0609665